11-1-2015

Recent advances in the use of mass spectrometry to examine structure/function relationships in photosystem II

Terry M. Bricker
Louisiana State University

Manjula P. Mummadisetti
Louisiana State University

Laurie K. Frankel
Louisiana State University

Recommended Citation

Bricker, T., Mummadisetti, M., & Frankel, L. (2015). Recent advances in the use of mass spectrometry to examine structure/function relationships in photosystem II. *Journal of Photochemistry and Photobiology B: Biology, 152*, 227-246. https://doi.org/10.1016/j.jphotobiol.2015.08.031

Recent Advances in the use of Mass Spectrometry to Examine Structure/Function Relationships in Photosystem II

Terry M. Bricker[1],Manjula P. Mummadisetti, and Laurie K. Frankel

Department of Biological Sciences, Division of Biochemistry and Molecular Biology, Louisiana State University, Baton Rouge, LA 70803

[1]Corresponding Author: Terry M. Bricker, Department of Biological Sciences, Division of Biochemistry and Molecular Biology, Louisiana State University, Baton Rouge, Louisiana 70803. Telephone: 225-578-1555, E-mail: btbric@lsu.edu

Key Words: photosynthesis, Photosystem II, tandem mass spectrometry, membrane proteins, chemical protein modification, protein-protein interactions

Abstract

Tandem mass spectrometryoften coupled with chemical modification techniques,are developing into increasingly important tools in structural biology. Thesemethods can provide important supplementary information concerning the structural organization and subunit make-up of membrane protein complexes, identification of conformational changes occurring during enzymatic reactions, identification of the location of posttranslational modifications, elucidation of the structure of assembly and repair complexes. In this review, we will present a brief introduction to Photosystem II, tandem mass spectrometry and protein modification techniques that have been used to examine the photosystem. We will then discuss a number of recent case studies that have used these techniques to address open questions concerning PS II. These include the nature of subunit-subunit interactions within the phycobilisome, the interaction of phycobilisomes with Photosystem I and the Orange Carotenoid Protein, the location of CyanoQ, PsbQ and PsbP within Photosystem II, the identification of phosphorylation and oxidative modification sites within the photosystem, etc. Finally, we will discuss some of the future prospects for the use of these methods in examining other open questions in PS II structural biochemistry.

1. Introduction

One of the central objectives of modern biochemical investigation is understanding the structural and functional interactions within membrane protein complexes. These complexes provide the basis for cellular interaction with the environment, intercellular interaction and communication, cell adhesion, inter- and intracellular transport of nutrients, and energy transduction processes. In all photosynthetic organisms, the harvesting of light energy and its conversion to biologically useful forms rely uniformly on ensembles of extrinsic and intrinsic membrane proteins. Since the initial report of the structure of the purple bacterial reaction center over thirty years ago [1, 2], X-ray crystallography has been extraordinarily successful at providing molecular structures for most of the membrane protein complexes involved in photosynthetic electron transport. These include the aforementioned purple bacterial reaction center, cyanobacterial Photosystem II (PS II,[3-7]), cyanobacterial and higher plant Photosystem I (PS I,[8, 9]), cyanobacterial and green algal cytochrome b_6/fcomplexes[10, 11] and the F_1 domain of ATP Synthase (although not from a photosynthetic organism [12]). X-ray crystallography has also provided critical information concerning the structure of a variety of both intrinsic [13, 14]and extrinsiclight-harvesting antennae components[15, 16]. Additionally X-ray crystallography and multidimensional nuclear magnetic resonance studieshave provided structures for a variety of isolated extrinsic protein subunits of photosynthetic complexes not presentin the current crystal structures of PS II. These include CyanoQ, PsbQ [17-20], CyanoP and PsbP[21-24]. The structures of a number of assembly factors for PS II includingPsb27[25],Psb28 [26], Ycf48 [27]and Psb31 [28]have been solved using these methods.Single particle imaging (and cryoelectron microscopy) has also contributed significantly to our understanding of photosynthetic supercomplexes such as the PS II-LHC II[29-33], PS I-LHCII[34], the PS II-phycobilisome [35]and PS I-phycobilisome [36, 37]interactions. Atomic force microscopy is also a developing technique which may be useful in this regard [38-40].

Recently, high resolution tandem mass spectrometry, coupled with site-specific chemical modification and/or protein crosslinking methodologies[41-43], is developing into a complementary technique for the structural examination of membrane protein complexes[41, 44]. These techniques provide low resolution structural information concerning the exposure of domains of constituent subunits to the bulk solvent and the identification of interacting domains of the protein subunits within a complex. This complementary information can be quite useful. X-ray crystallography provides high-resolution structural information of the protein complex in, necessarily, a single conformational state. Protein complexes, however, are often dynamic, assuming multiple structural states as their reaction mechanism progresses. While it is sometimes possible to use inhibitors to trap the protein complex in a reaction-specific conformational state (for instance, [45, 46]),often this is not possible. It is also assumed that the crystallizable form of a protein complex represents the *in vivo* structure. However, it must be recognized that crystallization conditions seldom replicate *in vivo* conditions with regard to ionic strength and make-up, pH, constituent lipids, etc.; all of which can affect structure. It should additionally be noted that weakly bound subunits may be lost from protein complexes during the crystallization process, which involves the use of detergents, non-physiological buffer conditions, high ionic or osmotic strength, etc. Posttranslational modifications of membrane protein complexes also occur. If these are present in the subset of the protein complexes that are crystallizable, the electron density at the site of modification will be proportionally decreased. It is also possible that the presence of a posttranslational modification could preclude (or even

potentiate) the formation of crystals. Finally,proteins that interact transiently (and usually relatively weakly) with membrane protein complexes cannot be identified using X-ray crystallography alone. All of these considerations can be addressed, at various levels, by mass spectrometry.

In this review, we will first briefly discuss PS II and some of the techniques that have recently been used to examine this membrane protein complex using mass analysis. This discussion will not be exhaustive and the reader will be directed to more authoritative and complete reviews on these specific topics. We will then discuss a number of recent case studies that have productively used mass spectrometry in the examination of the structure and function of PS II. Finally, we will discuss possible future experiments which can address long-standing problems in the field.

1.1 Photosystem II, Briefly

PS II functions as a light energy-driven water-plastoquinone oxidoreductase. In all oxygenic organisms, light is trapped by and funneled through light-harvesting pigment protein complexes (extrinsic phycobilisomesin cyanobacteria and red algae and light-harvesting chlorophyll (LHC) proteins in green algae, other algae and land plants) to the reaction center of PS II, which contains a special dimeric chlorophyll, P_{680}. After excitation, P_{680} becomes photooxidized and donates an electron to the primary acceptor of PS II, a protein-bound pheophytin. On the reducing side of the photosystem, this charge separation is further stabilized by the transfer of this electron first to Q_A and then to Q_B, protein-bound plastoquinones. The accumulation of two reducing equivalents on Q_B followed by protonation leads to the formation of plastoquinol, which is then released from PS II. Concomitantly, on the oxidizing side of the photosystem, P_{680}^+ is reduced by $Y_Z^{\bullet}$, a tyrosyl radical located on the D1 protein. The subsequent reduction of $Y_Z^{\bullet}$ leads to the accumulation of an oxidizing equivalent in the oxygen-evolving complex. The accumulation of four such oxidizing equivalents, in a manner consistent with the observed S-state transitions, leads to the release of oxygen from the complex. During the accumulation of these oxidizing equivalents, protons are released into the lumenal space of the thylakoid membrane (for reviews, see [47, 48]).

High resolution crystal structures are available for thermophiliccyanobacterial PS II [3-7], which contains seventeen intrinsic membrane protein components and three extrinsic membrane components (Fig. 1). The complex is a dimer with each monomer containing thirty-five chl *a*, two pheophytin *a*, two plastoquinones, two hemes and one non-heme iron. Each monomer also contains an oxygen-evolving site which consists of a Mn_4CaO_5 metal cluster associated with two chloride ions. Numerous carotenoids and lipids are also associated with the complex [6]. No crystal structures are available for the higher plant or green algal PS II, although these are generally assumed to be very similar to the cyanobacterial photosystem. However, it should be noted, that these systems contain two extrinsic subunits that are not present in cyanobacteria (PsbP and PsbQ) and that they lack the PsbU and PsbV subunits [49, 50]. Additionally, numerous lines of biochemical evidence indicate that there are two copies of the PsbO protein per PS II monomer in higher plants, whereas only one appears to be present in cyanobacteria [50, 51]. In all systems, PS II is highly susceptible to photoinhibition and *in vivo*the complex is continuously being assembled, disassembled and repaired [52]. Reactive oxygen species (ROS) modification of unidentified residues within the photosystem is thought to trigger the photoinhibitory process [53, 54]. For complete reviews on PS II structure/function the reader

should consult[55-58].

1.2Protein Mass Spectrometry, Briefly

In a typical tandem mass spectrometry experiment, protein complexes, proteins or peptides are ionized, mobilized into the gas phase and introduced into the mass spectrometer where the mass spectra of theseprecursor ions are acquired. Precursor ions,which are usually selected in a data-dependent manner, are then fragmented and the mass spectra of these product ions are acquired. Software is then used to examine the population of product ions observed to be derived from a specific precursor ion. These spectra are then compared by software to a target protein library where all possible precursor ions (and the product ions from each precursor) are examined. This analysis yields sequence information which can be used to identify precursor ions and determine the location of native posttranslational modifications and/or chemically introduced protein modifications.

Two different types of mass spectrometry experiments can be used to investigate the structural characteristics of proteins and their complexes. These are termed "Top-Down" and "Bottom-Up" experiments[59-61]. The terminology is based on the entities (intact protein/protein complexes vs. peptides) introduced into the mass spectrometer. In Top-Down experiments, intact proteins areexamined by mass spectrometry. A series of differentially charged ions are observed with different mass/charge ratios (m/z); this m/z envelope isdeconvoluted to give the mass of the intact complex. This mass includes the mass of the protein, cofactors, posttranslational modifications, lipids and detergents associated with the complex. The precursor ions (in this case, the intact protein)arefragmented (see below). This generates a population of productionsthat can be used in principal to determine the amino acid sequence of the parent protein(s) and also identifythe location of native posttranslational modifications and/or chemical modifications. In Bottom-Up experiments, proteins (often initially separated by polyacrylamide gel electrophoresis) are digested with site-specific proteases or chemical reagents and the resulting peptide fragments are resolved by reversed-phase chromatography followed by mass spectrometry. The precursor ions (in this case, proteolytic peptides of the target protein) are then fragmented yielding product ions (see below).Theseare then analyzed by a second round of mass analysis whichis used to determine the amino acid sequences of the precursor ions. The case studies discussed below have uniformly used a “Bottom-Up” strategy in their experiments.

While a variety of ionization methods are available for organic molecule mass spectrometry, two ionization methods are typically used to analyze proteins and peptides[62]. These are matrix-assisted laser desorption/ionization (MALDI) and electro-spray ionization (ESI). These are soft ionization techniques, which generally do not fragment the molecules under analysis and, under the appropriate conditions, maintain non-covalent interactions. In the studies that we will discuss, electro-spray ionization (ESI) was generally usually used as an ionization method.

Numerous types of mass spectrometers are available to analyze biological samples. For in-depth information, the reader should consult these excellent reviews [63-65]. Most of the recent studies examining PS II have utilized either Fourier transform ion cyclotron resonance (FTICR) or linear ion trap quadrupole-Orbitrap instruments (LTQ-Orbitrap) (both of these instrument types use Fourier transform algorithms to deconvolute the raw experimental data). The principal difference in these instruments is that in the case of FTICR, ions orbit in a

magnetic field generated by high-field superconducting magnets while in Orbitrap instruments the ions orbit in an electric field. Both offer extremely high mass accuracies and femtomole sensitivity (Table 1).

Several fragmentation techniques are available including collision-induced dissociation (CID), electron-capture dissociation (ECD), and electron transfer dissociation (ETD)[64]. In the studies that we will discuss, CID has been uniformly used. In CID, the precursor ions collide with gas ions which are at extremely low pressure; this leads to heating of the precursor ion and its fragmentation,principally at the labile C-N peptide bond. This yields one series of ions extending from the C-terminus towards the N-terminus (y^+-ion series) and a second series of ions extending from the N-terminus towards the C-terminus (b^+-ion series). Since the precursor ion is usually multiply charged, the product ions often also exhibit multiply charged states (for example, for a precursor ion in the +3 charge state, product ions may be observed bearing +3, +2 or +1 charges). In addition to these ions, the neutral loss of water, ammonia and labile posttranslational modification often occurs, giving rise to additional product ions. A typical, high quality mass spectrum obtained by ESI followed by tandem mass spectrometry using CID fragmentation is illustrated in Fig. 2. It should be noted that ECD and ETD fragmentation methods can offer significant advantages in the analysis of intact proteins and their complexes and in the examination of posttranslational modifications [64], but these methods are not generally available and have not been utilized in the examination of PS II.

In a typical tandem mass spectrometry experiment, thousands of mass spectra must be analyzed using computer software. Typically, theoretical tandem mass spectra are derived from each possible peptide present in a library of target proteins.Experimental spectra are then matched to the theoretical spectra for identification.Numerous software packages are available for the identification of proteins and the location of chemical and posttranslational modifications based on mass spectrometry data. A few of these include SEQUEST [66], MASCOT [67], GPMAW[68]and MassMatrix [69, 70]. Additionally, a number of programs are available to specifically examine particular types of chemical modifications, including chemical crosslinking patterns (xQUEST[71], pLink[72], Xlink[73], etc.) and oxidative modifications (ProtMapMS,[74]).In our laboratory [75-78], and several #6631}, MassMatrix[69, 70] has been used to identify site-specific chemical modifications, elucidate protein crosslinking patterns and examine posttranslational modifications. This software suite can either be implemented on personal computers or using the onlineMassMatrix Server(http://www.massmatrix.net). Both types of resources have been available free of charge. The reader is encouraged to carefully examine the literature concerning the myriad software implementations for examining mass spectrometry data, as a full discussion of this topic is well beyond the scope of this review. ss

One of the principal challenges in using mass spectrometryfor locatingprotein modificationsis the determination ofthe statistical significance of a particular peptide identification.The "p-value" is the most commonly used statistic in this regard. P-values provide an estimate of the probability that the null hypothesis is correct. Within the context of a mass spectrometry experiment, the null hypothesis is that acorrect peptide identification **was not made**using the available data and that an incorrect peptide identification occurred by chance. Consequently, a low p-value implies a low probability ofan incorrectpeptide identification [79]. P-values for specific peptide identifications must be chosen judiciously. For proteomics studies in which proteins are simply identified by the presence of their peptide sequence within a sample after screening large, often whole proteome libraries, a p-value of 0.05, which is the default p-value in MASCOT searches, is typically used (often with the further constraint that at least two

independent peptides be identified for a positive identification for a specific protein). When examining proteins for specific modifications, however, we feel that much more stringent criteria are appropriate. While the protein libraries being screened are usually much smaller, the number of possible modification sites is often very large. Additionally, multiple modifications may occur on the same peptide and the level of labeling at a particular site is usually highly variable, often only a few percent of the total peptide abundance. Also, unless enrichment procedures are available (for instance, the use of monomeric avidin to isolate biotinylated peptides), the yield of modified peptides may be quite low and present in a high background of unmodified peptides. When the yield of a modified peptide is low, the intensity of the observed ions may also be low and the noise level in the spectrum may become significant. While the number of putative identified modifications and/or crosslinked products will increase with higher p-values, the probability that these are correct identifications decreases.

In MassMatrix [70]peptide matches are determined by three statistical scores: pp, pp_2[69], and pp_{tag}[80].The pp score evaluates the probability that the **number** of matched product ions in an experimental spectrum could be the result of a random occurrence. The pp_2 score evaluates the probability that the total **abundance** of matched product ions in the experimental spectrum could be the result of a random occurrence. Finally, the pp_{tag}score evaluates the number of "sequence tags" in a peptide identification; these are consecutive y- and b-ion pairs which are used to determine peptide sequences. The more sequence tags present for a particular peptide identification, the higher the probability that the peptide match is correct. All of these values are influenced by the size of the protein database being searched (the larger the database, the higher the probability of incorrect peptide identifications) and the mass search tolerances for both the precursor and product ions (the larger the mass search tolerances, the higher the probability of incorrect peptide identifications) and the overall abundance of the target peptide.Fig.3 illustrates the quality of tandem mass spectrafor the same peptide at various p-values. As the p-values decrease, more of the predicted y- and b-ions and their neutral loss ion derivatives are detected. It is our view that the p-values of the peptides discussed in a paper should be provided, at the very least in the supplementary information. It is also our opinion that very rigorous p-values should be used for identification of protein modifications. In our laboratory, for large mass modifications, such as the identification of crosslinked peptides we use p-values $\leq 10^{-4}$; for small modifications, such as oxidations, we usep-values $\leq 10^{-5}$. It should also be pointed out that, in a particular experiment, the maximum p-value which will be considered significant fora positive peptide identification should be identified **before** the experiment is performed. Decoy libraries should also be examined in every experiment [81]. In these libraries the amino acid sequences for the target proteins are either in reversed order or are randomized. When searched within a mass spectrometry experiment, the results give an estimate of the number of false positive identifications within a particular data set. In MassMatrix, decoy libraries are automatically generated and searched and it is recommended that if the decoy% $\geq$ 2.5% for a particular protein identification, the mass search parameters be adjusted. In our laboratory the cutoff decoy% must be $\approx$0.0%. Finally, it is always preferable that multiple independent identifications of a particular modification feature be observed either within or across experiments, as this greatly increases the reliability of an identification.

It should also be pointed out that a variety of quantitative mass spectrometry techniques are available to examine to examine changes (either relative or absolute) in the amounts of proteins present in different biological states. These studies are beyond the scope of this review and the reader is encouraged to consult a number of excellent reviews on this topic [82, 83].

Only a few studies have used these techniques to examine structure/function relationships within PS II (for example [84-86]). It is our view that these techniques will become increasingly important in future studies of the photosystem.

1.3 Protein ModificationTechniques

A variety of protein modification chemistries can be used to modify amino acid residues, yielding mass changes which can be identified by mass spectrometry [87]. These reagents allow the identification of surface-exposed domains within protein complexes. In PS II, site-specific modification has been regularly used to investigate putative binding domains for the extrinsic subunits[88-95], however, only recently has the use of these labeling reagents been coupled to the use of tandem mass spectrometry to unambiguously identify modification sites[96, 97]. Two reagents (Fig. 4) which have been commonly used to study PS II include *N*-hydroxysuccinimidobiotin (NHS-biotin), which modifies the ε-amino group of lysyl residues and unblocked N-termini, and 1-ethyl-3-(3-dimethylaminopropyl)-carbodiimide· HCl (EDC), coupled with high concentrations of either glycine methyl ester or glycine ethyl ester, which modifies the carboxyl groups on aspartyl and glutamyl residues and C-termini. One major limitation of the use of these reagents is that they specifically modify only a limited subset of amino acid residues and consequently provide only limited information concerning exposed domains.

Radiolytic footprinting can provide a more global view of the surface-exposed features in large protein complexes [98]. This method relies on the production of $^{\bullet}OH$, a potent ROS species, upon exposure of water to X-rays produced by a synchrotron source. The lifetime of $^{\bullet}OH$ in bulk water is ≈1 ns during which time it can diffuse ≈10 Å.When generated in the bulk solvent, $^{\bullet}OH$ can modifya variety of surface-exposed amino acid residues. Fourteen amino acids are generally considered to be susceptible to such oxidative modification. The relative order of their susceptibility to oxidative modification is: Cys>Met >Trp>Tyr>Phe> His>Leu≈ Ile>Arg ≈ Lys ≈ Val>Ser≈ Thr ≈Pro[98]. Other amino acids can be modified but with lower reactivity.The oxidatively modified residues are then identified using tandem mass spectrometry and these oxidative modifications are mapped onto the crystal structures of the subunits. Recently, this technique has been used to map the surface exposed domains on PsbP and PsbQ bound to PS II [78]. Additionally, this is a useful method to identify buried water molecules in proteins [99]. We have used this technique to identify water channels leading to the active site of PS II and putative oxygen/ROS egress pathways from the active site. [76]. It should be noted that other methods can be used to generate $^{\bullet}OH$ for oxidative footprinting. These include Fenton chemistry [100], laser photolysis of H_2O_2[101]and pulsed electron beam water radiolysis [102].

Protein crosslinking has been used extensively in earlier studies to examine subunit-subunit interactions within PS II [89, 103-113] and recently this technique has been coupled to the use of tandem mass spectrometry to identify crosslinking sites [78, 114-119].Numerous reagents are available for protein crosslinking. These typically consist of reactive functional head group(s) at either ends of spacer arms of variable length and composition. Reaction of the head groups with amino acid R-groups (or, depending on the crosslinker, N- and C-termini) of spatially proximate amino acid residuesgenerates a covalent bond.The length of the spacer arm provides distance constraints between the crosslinked residues.Identification of the crosslinked residues allows the derivation oflow resolution 3D structure and distance maps of the target protein or protein complex[42, 120, 121] for which crystal structures are not available.

Additionally, chemical crosslinking is useful in preserving unstable or transient structural elements thatcannot be observed by X-ray and NMR methods. There are numerous commercially available protein crosslinkers with variable spacer arm length, homo- and heterobifunctionalhead groups, photoreactive head groups, crosslinkers which are membrane- permeable or impermeable, affinity-tagged crosslinking reagents, reagents which are cleavable by CID, etc. A full examination of the characteristics of these myriad protein crosslinkersis well beyond the scope of this review and the reader is encouraged to consult authoritative reviews on this topic [122-124].

Only a few of these reagents have been used in investigating the structure of PS II (Fig. 4). The most commonly used reagents contain *N*-hydroxysuccinimidyl(NHS) headgroups separated by spacer arms. Targets of these reagents include the ε amino group of lysyl residues and N-termini. Additionally, at pH 6.0 these can react with tyrosyl, seryl and threonyl residues, however, the seryl and threonyl crosslinked products are somewhat less stable [125, 126].Disuccinimidylsuberate (DSS) contains an eight-carbon spacer arm and is hydrophobic. Typically, hydrophobic crosslinkers are dissolved in DMSO prior to use. Dithiobis(succinimidyl propionate) (DSP) is a hydrophobic,cleavable NHS ester crosslinker, with eight carbon spacer arm containing a disulfide bond. Bis(sulfosuccinimidyl)suberate (BS3, also known as Sulfo-DSS), is a hydrophilic, homobifunctional reagent containing an*N*-hydroxysulfosuccinimide ester headgroup separated by an eight-carbon spacer arm and is similar to DSS. 3,3'-dithiobis(sulfosuccinimidyl propionate (DTSSP) is the sulfonated form of DSP, and is also hydrophilic. The hydrophilic crosslinkers cannot penetrate biological membranes while the hydrophobic crosslinkers can penetrate these membranes and, consequently, are useful for *in vivo* protein crosslinking.

EDC is a hydrophilic,zero-length, heterobifunctional, carbodiimide crosslinker, which activates carboxyl groups and subsequently reacts with primary amines with the elimination of isourea. This reagent is typically used in the pH range of 4.5 - 7.2. Only residues which are in van der Waals contact are crosslinked with this reagent. Sulfo-NHS is often added to the crosslinking reaction along with EDC, which generates a more stable reaction intermediate and yields higher crosslinking efficiencies.

Gluteraldehyde reacts with lysyl (and N-termini), tyrosyl, tryptophanyl, phenylalaninyl, histidyl, cystinyl, prolyl, seryl, glycyl and arginyl residues and is widely used for protein immobilization[127]. Numerous forms of gluteraldehyde are present in aqueous solution and its mechanism(s) of crosslinking is unclear [127]. Recently this reagent, in combination with tandem mass spectrometry, has been used in examining phycobilisome subunit interactions [119]. It should be noted that formaldehyde, which exhibits similar amino acid residue reactivity[128],has been extensively used in mapping protein-DNA interactions[129, 130]and is developing into a useful reagent for mapping protein-protein interactions [128, 131, 132], particularly for*in vivo* applications.

2. Case Studies

2.1 Cyanobacterial Photosystem II

2.1.1 Phycobilisome Structure and Interactions with PS I and PS II

Phycobilisomes are enormous extrinsic membrane protein complexes (>5 MDa) which are the principal light-harvesting antennae in cyanobacteria and red algae, facilitating light absorption typically in the 500-650 nm region.In cyanobacteria and red algae, the structure of phycobilisomes and the mode of interaction between the phycobilisomes and the photosystems has been the subject of much study (for reviews see [133-135]). The phycobilisome contain numerous colored proteins (α and β subunits of allophycocyanin (APC), phycocyanin (PC), and phycoerythrin (PE), etc.) as well as numerous colorless linker polypeptides. The precise subunit composition of the phycobilisome is highly species-specific. The overall structure of phycobilisome has been studied using conventional electron microscopy and, more recently,single particle analysis [35, 136]. These studies indicate that the overall architecture of the phycobilisomecontains a variable number of rod elements containing PC, PE, etc. attached to an APC corethat then associates with the photosystems. The subunit-subunit interactions within the phycobilisome, however,remain quite unclear [137, 138]. While many of the individual subunits have been analyzed by X-ray crystallography, most at near atomic resolutions, the interactions between these structural elementsremainpoorly understood. This in large measure is due to the instability of the phycobilisome in the absence of typically very high concentrations of phosphate, which significantly complicates purification and analysis of the intact phycobilisome.

From a functional perspective, it had been shown using 77 K fluorescence excitation experiments,that energy trapped by the phycobilisome could be efficiently transferred to both PS II and PS I reaction centers[139]. Under conditions where all of the PS II traps were open, 90% of the excitation energy was transferred to the PS II reaction center; under conditions where the PS II traps were closed, 50% of the excitation energy was transferred to PS I reaction centers. It was unclear, however, if the excitation energy transfer to PS I was indirect, via the interior PS II chl *a* antennae ([140, 141], phycobilisome→ PS II chl *a* antennae → PS I chl *a* antennae), direct ([142, 143], phycobilisome → PS I chl *a* antennae) or in-parallel ([144], PS II chl *a* antennae ← phycobilisome → PS I chl *a* antennae)(for an in-depth discussion, see [135]). Interestingly, treatment of intact cells with N-ethylmaleamide disrupted energy transfer from phycobilisomes to PS I without affecting energy transfer to PS II [145] although the subunits and residues modified by this treatment were not identified. This could indicate the involvement of specific cystinyl residues in the energy transfer.

Tal et al. [119] have recently examined the subunit-subunit interactions within the isolated phycobilisome of *Thermosynechococcus vulcanus* using protein crosslinking and tandem mass spectrometry. These authors observed and mapped numerous crosslinked residues, using BS3 and gluteraldehyde, at the phycobilisome subunit interfaces. Those with the lowest p-values are illustrated in the interaction map shown in Fig. 5 and includecrosslinked residues within the C-phycocyanin$(\alpha\beta)_3$trimer(CpcA:^{2}K-CpcB:^{78}R and CpcA:^{32}K-CpcB^{7}K), at the phycocyanin-allophycocyanin interface(CpcA:^{83}K-ApcA:^{36}R, CpcB:^{37}R-ApcA:^{36}R and CpcB^{36}K-ApcB^{26}K), and between the linker polypeptide CpcG2 and the "minor" allophycocyanin core cylinder component ApcF (CpcG2:^{182}R-ApcF^{26}R and CpcG2:^{164}R-ApcF^{21}R). The analysis of these and numerous other crosslinked species (which were identified at higher p-values), in combination with protein modeling of the subunits for which X-ray crystallographic data was not available, allowed these authors to present detailed maps of the subunit-subunit interactions within the phycobilisome complex. These results provide critically important testable hypotheses concerning the overall subunit interactions within the phycobilisome.

Recently, in *Synechocystis* 6803 Liu et al. [115] have isolated a functional supercomplex (PS II–phycobilisome–PS I) composed of PS II, PS I and the phycobilisomeantennae complex.

Isolation of this complex was facilitated by *in vivo* crosslinking with the membrane permeanthomobifunctional crosslinkers DSP and DSSP, which apparently stabilize the interactions between these three complexes, and the use of His-tagged PS II complexes [146]which allowed the isolation of the supercomplex by metal affinity chromatography.Within the PS II– phycobilisome–PS I supercomplex the stoichiometry of the individual subcomplexes appears to be 1:1:1. These authors demonstrated that the phycobilisomes were energetically coupled to both PS II and PS I and that both photosystems were activewith respect to electron transport within thissupercomplex. The interaction between PS I and the phycobilisome (Fig. 6A) appears to be mediated by crosslinks between ApcB and PS I (ApcB:^{17}K-PsaA:^{30}K and PsaD:76K) and ApcD and PS I (ApcD:^{48}K-PsaA:^{11}K and ApcD:^{49}K-PsaD:^{76}K). A crosslink between the phycobilisome linker polypeptide CpcC2 and PsaF (CpcC2:^{256}K-PsaF:^{92}K) was also observed. The structural interaction between PS II subunits and the phycobilisome(Fig. 6B) appears to be mediated by the ApcE and several PS II subunits:PsbB (ApcE:^{87}K-PsbB:^{227}K), PsbC (ApcE:^{523}K-PsbC:^{457}K and ApcE:^{584}K-PsbC:^{457}K), PsbD (ApcE:^{317}K-PsbD:^{23}K) and PsbI (ApcE:^{523}K-PsbI:^{35}K).

It is unclear from this study, however, what proportion of PS II and PS I present *in vivo*isactually associated with this supercomplex. It is possible that only a small proportion of the phycobilisomes are simultaneously associated with both PS II and PSI, and that the supercomplex isolated by Liu et al. [115] was a transient association trapped by the crosslinking process. It must be noted, however, that no PS II–phycobilisome or PS I–phycobilisomesupercomplexes were observed in this study. One might expect that these putative forms would also be stabilized by treatment with the crosslinker and these should have been observed if the PS II–phycobilisome–PS I supercomplex existed only transiently. Interestingly, in *Anabaena*, a novel phycobilisome–PS I supercomplex has recently been described [37]which lacks allophycocyanin and a number of linker polypeptides, but contains the linker polypeptide CpcG3 (CpcL), which was not observed in the PS II–phycobilisome–PS I supercomplex [115]. It is not known if this architecture is generally found in cyanobacteria or if it is an adaptation specific for some nitrogen-fixing strains.

2.1.2 Orange Carotenoid Protein

In cyanobacteria, under high intensity blue-green light illumination, a dark-reversible drop in the fluorescence yield of PS II is observed related to NPQ[147]. The observed fluorescence quenching is present in mutant strains which lack the PS II reaction center but contain phycobilisomes[148], however the quenching isabsent in mutants which lack phycobilisomes[149] but contain PS II reaction centers. This phycobilisome-centered fluorescence quenching is termed qE_{cya} and mechanistically is related to the binding of a water-soluble carotenoid-containing protein, called the orange carotenoid protein (OCP), to the phycobilisome[149]. This protein, originally identified by Holt and Krogmann[150], binds the carotenoid 3′-hydroxyechinenone [151]and undergoes a reversible conformational change when exposed to blue light. The OCP^o form binds weakly to phycobilisome; upon exposure to blue-green light it converts to the OCP^r form, which binds to the phycobilisome and quenches fluorescence. In the dark, OCP^r binds the fluorescence recovery protein (FCP), which accelerates the conversion of OCP^r to OCP^o (for an excellent review of the OCP, FRP and their interactions see [152]).Structures for both the OCP (PDB:3MG1[153]) and FRP (PDB:4JDX[154]) are available.

Recently, important work from the Blankenship laboratory has identified both structural rearrangements occurring in the OCP during the OCP^o to OCP^r transition [97, 118]and the binding location for the OCP^r form to the phycobilisome[118]. Under native electrospray ionization (nESI) conditions intact protein complexes can be examined[155]. When the dark-adapted OCP^o form is examined by gentle nESI,both monomer and dimer states are observedin a ≈1:1 ratio which suggests that these two forms exist in a 1:1 equilibrium in the OCP^o state[118], at least *in vitro*. Upon blue-green light illumination, and OCP^o to OCP^r conversion, the monomer to dimer ratio is ≈5:1, indicating that the equilibrium has been shifted strongly to the monomeric form. After a subsequent 30 min dark incubation a monomer to dimer ratio of ≈5:4 was observed, which indicated a return to the OCP^odark equilibrium state. Collision-induced dissociation and ion mobility measurements were also performed which examined the loss of 3′-hydroxyechinenone from the monomeric and dimeric states. It was found that the pigment was more resistant to dissociation in the dimeric state than the monomeric state, indicating a more open structure for the protein in the OCP^r form.Taken together, these results indicate that the active OCP^r form of the protein is the monomer. It is hypothesized that absorption of light energy by the carotenoid leads to conformational changes in the pigment that in turn elicits conformational rearrangement in the protein. These protein conformational changes then lead to the dimer ⦿ monomer transition, with the monomer associating with the APC core subunits.

Protein crosslinking coupled with mass spectrometry has also been used to identify the interacting domains between the OCP^r form and the phycobilisome (Fig. 7), at least *in vitro*[118]. Isolated phycobilisomes were incubated with OCP^o, illuminated to produce OCP^r, and the phycobilisome-OCP^r complex was isolated. This *in vitro* model of the phycobilisome-OCP^r interaction had been previously well characterized [156]. The protein crosslinkers BS3 and DSS were used in these studies. As expected, no crosslinked species were observed between the OCP and the PC rod elements. Three OCP-APS crosslinked species were observed, OCP:^{167}K-ApcB:^{58}K, OCP^{249}K−ApcB:^{26}K, and OCP:^{170}K− ApcE:^{4}K.These interactions are illustrated in Fig. 7A. The observation of these crosslinked species allowed the investigators to model the OCP-APC interaction. They hypothesize that OCP^r is associated with the basal cylinders of the allophycocyanin core, that the N-terminusof the OCP appears buried between two APC trimers (one APC_{660} and one APC_{680}), and that the C-terminus is solvent-exposed. One prediction that can be made from this model is that there maybe only two OCP^r binding sites per phycobilisome. This prediction remains to be tested. It would be very interesting if *in vivo* crosslinking experiments could be performed in this system. Additionally, experiments analogous to those described above could possibly be performed with OCP^r and the FRP. One would predict that FRP might facilitate OCP dimer formation.

The conformational changes that occur during the OCP^o to OCP^r transition [97]have also been studied using the site-specific modification of carboxylates (Fig. 7B) with EDC and glycine ethyl ester hydrochloride (GEE).At high concentrations of GEE, the carboxylate-labeling reaction is much more favorable than the protein crosslinking reaction of EDC, alone. These investigators examined three different light conditions, darkness (OCP^o), continuous light (OCP^r) and intermittent light (mixture of OCP^o + OCP^r). In general, the labeling pattern of the OCP under intermittent light was intermediate between that observed under darkness and constant illumination. Interestingly, carboxylate modification of OCP under illumination stabilizes the OCP^r form and prevents recovery of the OCP^o form in the dark, at least in the absence of the FRP. It appears that modification of particular residues in the OCP^r state prevents the monomer ⦿dimer dark transition.Two groups of residues were identified which exhibited differential

labeling (Fig. 7B). One group exhibited increased labeling in the OCP^r state. These residues were located at the interface of the N- and C-terminal domains of the protein (^{19}D, ^{174}E and ^{244}E) and at the β-sheet core which, in the crystal structure, interacts with the N-terminus of the protein (^{6}D,^{258}E, ^{261}E, ^{262}E, ^{304}D and ^{311}D). The labeling of these residues indicates that these portions of the OCP exhibit greater solvent exposure in the OCP^r state. A second group of residues exhibited decreased labeling in the OCP^r state (^{65}E, ^{115}E and ^{118}E) and consequently, less solvent exposure. While the labeling features of some of these residues appear consistent with the dimeric crystal structures and the hypothesis that the OCP^r form is monomeric (for instance the increased labeling of ^{6}D and ^{19}D), the labeling features of the other residues are more difficult to explain and clearly require furtherstudy.

Recently,solvent accessibility changes upon the $OCP^o$to OCP^r conversion have been examined by radiolytic footprinting [157]. Residues near the N-terminus, ^{41}W, ^{42}F, ^{44}Y and ^{47}M, exhibited decreased solvent exposure upon conversion to the OCP^r form. Residues near the C-terminus, ^{276}P, ^{277}W, ^{278}F and ^{284}M, exhibited increased solvent exposure. Overall, the increase in solvent accessibility of the C-terminal domain and decrease in accessibility of the N-terminal domain appearquite consistent in both the radiolytic and chemical [97] footprinting experiments (Fig. 7B).

2.1.3 Location of CyanoQ within Cyanobacterial PS II

Cyanobacteria (and red algae) contain homologues of the higher plant PS II subunits PsbP and PsbQ [50, 158]. These proteins, CyanoP and CyanoQ, however are not present in any cyanobacterial crystal structure available. While the constitutive association of CyanoP with cyanobacterial PS II and its function is controversial[159-161], CyanoQ is a constitutive subunit of cyanobacterial PS II [162] which is lost during crystallization [161]. CyanoQ may also serve as an assembly factor, as multiple copies of CyanoQ are present in a late cyanobacterial PS II assembly complex [163].

The interaction of CyanoQ with other cyanobacterial PS II subunits and aproposed structural organization for this component within the complex has recently been presented by Liu et al. [117]. In these studies, the crosslinkers EDC, DTSSP and BS3 were used to modify PS II which had been isolated by metal affinity chromatography (via introduction of a polyhistidine tag on the C-terminus of CyanoQ [162]). A number of inter- and intraprotein crosslinked products were observed (Fig. 8A). CyanoQ was found to be crosslinked to both PsbO (CyanoQ:^{120}K-PsbO:^{180}K and CyanoQ:^{120}K-PsbO:^{59}K) using DTSSP (or BS3) and PsbB (CyanoQ:^{102}K-PsbB:^{440}D) using EDC. The identification of these crosslinked products allowed placement of CyanoQ adjacent to both PsbO and PsbB. Interestingly, two types of intraprotein crosslinked products were observed involving CyanoQ. Some of these were fully consistent with the observed crystal structure of CyanoQ(CyanoQ:^{96}K-CyanoQ:^{100}K, CyanoQ:^{100}K-CyanoQ:^{106}K, and CyanoQ:^{102}K-CyanoQ:^{106}K). One, however, cannot be explained within the monomeric CyanoQ structure. This crosslinked productCyanoQ:^{96}K- CyanoQ:^{120}K spansa distance of 41 Å, as these residues lie on opposite ends of a long α-helix. Either an unprecedented conformational change must occur upon binding of CyanoQ to the photosystem, bringing these residues in close proximity,or the observed crosslink occurs between two different molecules of CyanoQ which associate as asymmetrical, antiparallel dimer (Fig. 8B). The authors proposed a model for the interaction of the dimeric CyanoQ with cyanobacterial PS II in which a CyanoQ dimer(one from each PS II monomer) associates with the lumenal face of the

cyanobacterial PS II dimer, witheach copy of CyanoQ associating with both PsbO and CP 47 within each monomer.

2.2 Higher Plantand Green Algal Photosystem II

2.2.1 Location of PsbP and PsbQ in Photosystem II

One persistent problem in the study of higher plant PS II has been the absence of structural information concerning the location of PsbP and PsbQ. These components provide critical support for oxygen evolution by maintaining the association of the essential inorganic cofactors calcium and chloride with the photosystem at physiological ion concentrations [50]. It has also been suggested that PsbP may act to supply manganese to the photosystem during metal cluster assembly [24, 164, 165].Earlier, cryoelectron microscopy and single particle analysis were used to address this problem[30]. In that study, the X-ray structure of spinach LHCII and the cyanobacterial PSII crystal structure were overlaid onto a 17 Å projection map for PSII-LHCII from spinach [166]. This analysis indicated that PsbP interacts with PsbO andmay be locatedadjacent to CP43 and that PsbQ bridges the PsbO and PsbP proteins.

Nagao et al. [113] used EDC crosslinking and MALDI-TOF mass spectrometry to examine the interaction of the extrinsic proteins with *Chlamydomonas* PS II. This study was the first to indicate that PsbP was in van der Waals contact with PsbE, the α-subunit of cytochrome b_{559}. The authors, however, could not identify the site of this interaction due to the lack of fragmentation information in their experiments.Ido et al. [167] resolved this question using tandem mass spectrometry and EDC crosslinking of spinach PS II membranes. In these experiments the crosslinked residues PsbP:^{1}A-PsbE:^{57}E wereclearly identified in multiple independent spectra.

Recently, Ido et al.[116]used protein crosslinking and tandem mass spectrometry to further examine the location of PsbP and PsbQ in spinach PS II membranes. In this study, the authors used biotin-labeled PsbP and PsbQ proteins that were reconstituted with salt-washed PS II membranes prior to crosslinking with EDC. This allowed the affinity isolation of crosslinked products which contained either biotin-PsbP or biotin-PsbQ. The authors immunologically identified crosslinkedproducts which containedbiotin-PsbP in independent association withPsbE, PsbR,CP 43, and CP 26 and were able to map the crosslinked residues. Immunologically identified crosslinked products between biotin-PsbQ and CP 43 and CP 26 were also identified, however, the participating crosslinked residues could not be determined. After cleavage with trypsin or chymotrypsin, tandem mass spectrometry was able to identify the crosslinked residues for a subset of these associations (Fig. 9A). The interaction ofPsbP:^{1}A-PsbE:^{57}E, which had been described earlier [167], was verified. Additionally, the locations of novel crosslinking sites were determined. A crosslink interaction between PsbP:^{27}K-PsbR:^{22}D was identified. Anovel tertiary crosslinked product involving two PsbP peptides and a single CP 26 peptide was also observed (PsbP:^{115}E-PsbP:^{173}K -- PsbP:^{174}K-CP 26:^{96}E). These results indicated that PsbP is in van der Waals contact with PsbE, PsbR and CP 26. A model was presented in which PsbP, PsbQ and PsbR, are all associated with the periphery of the PS II complex near the membrane surface with PsbR adjacent to PsbE, PsbP adjacent to PsbR and PsbQ adjacent to PsbP and also associated with CP 43. In this model, the association of PsbP:^{1}A with PsbE:^{57}E requires that the N-terminus of PsbP be highly extended since PsbR occupies a position between PsbP and PsbE within the complex. It had earlier been demonstrated that the N-terminal 19 amino acids of PsbP were critical for stable binding and promotion of oxygen evolution activity ([168, 169]; for a

review of the structural and functional characteristics of PsbP, see [50, 158]). This important domain on PsbP, however, is not resolved in the available crystal structures [23, 24, 170]. Additionally, while PsbP and PsbQ were proposed to directly interact, neither protein is in direct contact with PsbO;both, however, appear to interact with CP 26.

Our laboratory also has examined these interactions using tandem mass spectrometry and the protein crosslinker BS3. Additionally, radiolytic footprinting was used to examine the domains on these proteins exposed to the bulk solvent [78].In this study we used the homobifunctional crosslinker BS3 which crosslinks lysyl residues, free N-termini and, at low pH, tyrosyl residues [120, 171, 172] which are within 11.4 Å. The crosslinked products were analyzed by tandem mass spectrometry. Critically, with respect to the Ido et al. model [116], we identified nine independent crosslinked products indicating that the N-terminal domain (^{1}A-^{40}K) and C-terminal domain (^{170}K-^{186}A) were closely associated. These interactions could not be identified when unbound PsbP was exposed to BS3 in solution. These crosslinks placed strong distance constraints on the N- and C-termini and allowed us to model the N-terminus of PS II-bound PsbP as a very compact structure which does not contain a long N-terminal extension. These findings help explain the observation that the N- and C-terminal domains cooperate in facilitating PsbP function in support of PS II activity[167]. Additionally, we identified two independent crosslinked products between PsbP and PsbQ(PsbP:^{96}K and PsbP:^{93}Y were crosslinked to PsbQ:^{1}E, Fig. 9A). PsbP:^{96}K and PsbP:^{93}Y both are located in a long, apparently mobile loop which was not resolved in the crystal structures available at the time of publication. Recently, Cao et al. [24] demonstrated that in the presence of bound manganese, this loop assumed a stable structure which is consistent with our observed crosslinking interactions (Fig. 9B).We also observed two independent crosslinkedproducts which indicated that PsbQ can form dimers when bound to the photosystem. PsbQ:^{98}K and PsbQ:^{101}K can both be crosslinked to PsbQ:^{133}Y. These crosslinked residues are separated by 30 Å and consequently could not be crosslinked using BS3 within the monomeric protein. This is highly reminiscent of the finding in cyanobacterial PS II that CyanoQ is present as an antiparallel homodimer[117], although the dimer we observed is not fully symmetric (Fig. 9C). Finally, we used radiolytic oxidative labeling to identify surface-exposed residues on PS II-bound PsbP and PsbQ. These results were consistent with earlier reports using site-specific chemical modification techniques [93-95]. Additionally, we identified a domain on PsbP that was shielded from oxidative modification and which was adjacent to the PsbP-PsbR binding site (PsbP:^{27}K-PsbR:^{22}D) identified by Ido, et al. [116]. This may define the surface interaction between these two subunits. Recently, Ifuku [173] has integrated these new findings into an updated model for the interaction of PsbP and PsbQ with higher plant PS II.

2.2.2 Experimental Identification of Putative Water and Oxygen Channels within PS II

Since the Mn_4O_5Ca oxygen-evolving site is buried within the protein matrix, channels which can transit substrate water to the metal cluster and which can vector product oxygen and protons away from the active site are necessary. A number of possible water/oxygen/proton channels within the photosystem have been proposed (for an excellent review see, [174]). These hypotheses have been based largely on computational studies using CAVER analysis [175], surface contact area analysis [176],or water streamline tracing coupled with molecular dynamic simulations [177, 178]. Briefly, at least four channels have been identified computationally as leading from the lumenal surface of PS II to the Mn_4O_5Ca cluster. These have been designated [174]: 1. "Back Channel",which was proposed to transport either oxygen [179] or water [176,

180], 2. "Narrow Channel",which may transport protons [176, 180], 3. "Broad Channel", was hypothesized to transport water and/or protons [176, 179, 180], and 4. "Large Channel", which was proposed to transport water and/or protons [179] or possibly oxygen [176, 180]. Limitations exist, however, with all of these largely computational studies which examine static crystal structures [176, 179, 180]; they fail to take into account molecular motion on the ns time scales which could substantially alter the overall shape and dimensions of the identified water channels within PS II. It should be noted that Vassiliev et al. [177, 178] have partially addressed this problem using molecular dynamic simulations of water movement within the photosystem. It has also been implicitly assumed in these studies that no conformational changes occur in the PS II structure during normal S-state transitions whichcould affect water transport to the active site or oxygen/protons away from the active site. It has been noted that even a modest conformational change involving one or a few amino acid residues could hypothetically either open or close putative water/oxygen/proton channels during S-state cycling [178].

In our laboratory, we hypothesized that the water present in channels leading to or possibly from the active site would be susceptible to radiolytic footprinting and we have used this technique to identify buried amino acid residues associated with such channels[76].In this experiment, spinach PS II membranes were exposed for various lengths of time (0-16 s) to synchrotron radiation. After irradiation, the samples were resolved bynon-oxidizing LiDS-PAGE and a subset of proteins (D1, D2, CP 43 and CP47) were isolated, digested with trypsin and analyzed by tandem mass spectrometry. MassMatrix [69, 70] was used to identify oxidatively modified residues and these were mapped onto the cyanobacterial PS II structure [6]. This analysis is feasible due to the strong predicted sequence and structural similarity of these proteins in the cyanobacterial and higher plant systems.

As expected, numerous surface residues on these PS II subunits were oxidatively modified. Additionally, a large number of modified buried residueswere observedover the experimental time-course. These modified residues fell into two groups(Fig. 10). The first group(Fig. 10A) was composed of numerous residues found in D1, D2 and CP 47 (D1 residues ^{331}M, ^{332}H, ^{333}E, and ^{334}R; D2 residues ^{323}E and ^{326}R, and CP47 residues ^{359}M, ^{363}F,^{364}E, ^{365}S, ^{425}I and^{426}F). The residues modified by irradiation formed a near continuous group of residues leading from the surface of the complex to the manganese cluster. Comparison of these residues with those found in Channels 1-4 (described above)indicated that 55% of the residues explicitly identified as forming the "Broad Channel" [174] exhibited oxidative modification; in the other channels 20-30% of the residues were modified. These experimental observations strongly support the hypothesis that the "Broad Channel" is a major source of substrate water supplying the active site of PS II. A second group (Fig. 10B) of buried residues was found solely on CP 43. This group includes the oxidized residues ^{354}E, ^{355}T, ^{356}M and ^{357}R, which were observed to be oxidized in the absence of irradiation, and which had previously been hypothesized to form part of an oxygen/ROS exit pathway from the manganese cluster to the surface of the photosystem (see section 2.2.4, [75]), and the residues ^{343}R, ^{348}E, ^{361}F, ^{366}L, and^{363}G, which were modified by irradiation. These residues also form a near contiguous pathway leading from the Mn_4O_5Ca cluster to the lumenal space. No computationally identified channels have been proposedin this domain of CP43. Many of these residues, however, are in contact with noncontiguous cavities that are present in CP43 and at the CP43-PsbO interface. It is possible that these residues constitute a previously unidentified water pathway within the PS II complex, particularly if conformational changes occur in this region during S-state cycling. An alternative hypothesis is that these modified CP 43 residues are adjacent to a pathway for oxygen and/or

ROS egress from the active site. These and other possible hypothesizes cannot be differentiated at this time.

2.2.3 Identification of Posttranslational Modifications in PS II- Phosphorylation

The earliest identification of posttranslational modifications of PS II using mass spectrometry was the identification of the phosphorylation sites on D1, D2 and CP43 by John Bennet's laboratory in 1988 [181]. Earlier, using the Edman degradation technique, this laboratory had demonstrated that PsbH was N-terminally phosphorylated, however the N-termini of D1, D2 and CP43 were blocked[182]. To identify the phosphorylation sites on these three components, the authors used techniques which are still routinely in use27 years later. After tryptic digestion the phosphorylated peptides were isolated by metal affinity chromatography, the peptides were resolved by HPLC on reversed phase columns, and analyzed on both triple quadrupole(using CID fragmentation) and tandem quadrupole (using laser photodissociation) Fourier transform mass spectrometers.D1 and D2 were both phosphorylated on *N*-acetyl-^{2}Thr while CP 43 was phosphorylated on *N*-acetyl-^{15}Thr. Thus, four different types of posttranslational modifications were observed in these proteins: removal of the *N*-formylmethionyl residue encoded by the initiation codon, removal of an additional thirteen N-terminal residues in the case of CP 43, N-terminal acetylation of the processed proteins, and phosphorylation of the N-terminal threonyl residues. Subsequent studies, using similar methodologies, identifiedthe phosphorylation sites of the LHC proteins in *Arabidopsis thaliana* (henceforth, *Arabidopsis*)[183, 184]and *Chlamydomonasreinhardtii*(henceforth *Chlamydomonas*)[185], an additional phosphorylation site on PsbH (^{4}T, [183]), and demonstrated that PsbR was a phosphorylation target, at leastin *Chlamydomonas* (^{15}S of the mature protein, [185]). These studies proved the general utility of these techniques. For authoritative reviews on the environmentally regulated reversible phosphorylation of PS II subunits, the reader should consult [186-188].

Additionally, the extrinsic proteins PsbP and PsbQ may be phosphorylated. While no phosphorylation of these subunits has been reported using standard radiolabeling procedures in any system, two *Arabidopsis* globalphosphoproteomic studies have identified putative phosphorylated peptides from these components after metal affinity chromatography or TiO_2 enrichment for phosphopeptides[189, 190]. Both PsbP-1 and PsbP-2 were reported to contain multiple phosphorylation sites (^{56}T, ^{66}T, ^{70}S and ^{82}S). No phosphorylated peptides were identified for PsbQ-1.However, phosphorylation of the PsbQ-2 protein at ^{91}S was reported. PsbP and PsbQ phosphorylation was detected under both dark and light incubation conditions. Earlier, the *Chlamydomonas* PsbQ protein had been identified in a phosphoproteomic study [191]as being phosphorylated at three sites, ^{117}T, ^{120}S, and ^{1121}T.The protein kinases and phosphatases associated with the putative phosphorylation on these extrinsic subunits have not been identified and the biological role played by the phosphorylation remains undetermined.

2.2.4Oxidative modifications

PS II is the major site of photoinhibition in all oxygenic organisms and appears particularly susceptible to damage by ROS [53, 54]. Briefly, it is hypothesized that ROS production at an unidentified site or sites within the photosystem leads to oxidative modification of largely unidentified amino acid residues within the complex. This damage affects structure and function withinPS II and initiates a signal transduction pathway which leads to the migration

of the damaged complex to the stroma thylakoids, partial disassembly of the complex, removal and replacement of the D1 protein with subsequent reassembly and migration of the fully repaired functional complex to the grana thylakoids. These processes require multiple repair and assembly factors which interact with PS II in a highly orchestrated manner[192]. For extensive reviews on this complex topic, the reader should consult [193-195] and for an alternative viewpoint, see [196, 197]. So, where are the sites of ROS production in PS II? The production of molecular oxygen by PS II is accompanied by the unavoidable possibility of oxidative modification of amino acid residues within the PS II complex in the vicinity of the Mn_4O_5Cametal cluster[53, 54]. Damaged manganese clusters may also contribute to ROS production by releasing partially oxidized water species (O_2^-, H_2O_2, $^{\bullet}OH$). Singlet oxygen (O_2*) produced at P_{680}, the primary electron donor of the photosystem, has also been proposed as a source of ROS generated by the photosystem [198-200]. Additionally, reductants produced by PS II, such as Q_B^{-2}[201], $Pheo_{D1}^-$[202], Q_A^-[203], and, possibly, reduced low potential cytochrome b_{559}[204, 205], appear to have redox potentials and lifetimes sufficient to partially reduce molecular oxygen, producing O_2^-, H_2O_2, and/or $^{\bullet}OH$. These sites have been hypothesized to be sources of ROS on the reducing side of the photosystem. Little progress has been made, however, in determining the relative importance of these multiple putative ROS production sites and only recently has a subset of oxidatively modified residues been identified. It is unclear which, if any, of the modified residues trigger PS II turnover and repair.

We have hypothesized that amino acid residues in the vicinity of the sites of ROS production would be particularly susceptible to ROS modification [75, 77]. The identification of such oxidatively modified residues in PS II should serve to identify both the sites of ROS generation, their relative importance in the photoinhibitory process and, possibly, help define the putative paths for ROS exit from PS II.Recently, the use of mass spectrometry has provided the first insights into the location of oxidatively modified residues within PS II. If our hypothesis is correct, then the identification of these residues suggests sites within the photosystem producing ROS.It should be noted, however, that the type of ROS which is responsible for a particular oxidative modification cannot be readily determined by mass spectrometry, alone.

In an early mass spectrometry study, Sharma et al. [206] identified six peptides on D1 and four peptides on D2 which contained oxidative modifications, some of which bore multiple oxidative modifications. While they identified the location of these peptides within, the proposed structures at that time of D1 and D2,they could not identify the modified residues within these peptides due to the lack of CID information. We have recently confirmed and extended this observation using CID fragmentation and identified several natively oxidized amino acid residues (D1:^{130}E, ^{133}L and ^{135}F) in close proximityto $Pheo_{D1}$[77]. D1:^{130}E is in van der Waals contact with the pheophytin and the other residues are within 13.8 Å. Additionally, other natively oxidized residues (D1:^{239}F, ^{241}Q, ^{242}E and D2: ^{238}P, ^{239}T, ^{242}E and ^{247}M) were in close proximity with Q_A [77]. D2:^{247}M is located 3.7 Å from the quinone and the other residues are within 13.5 Å (all measurements using the Umena PS II structure [6] as a model). These natively modified residues are illustrated in Fig. 11. These findings support the hypothesis that $Pheo_{D1}$ and Q_A could serve as sources of ROS on the reducing side of PS II. It should be emphasized, however, that these residues were identified in PS II isolated from field grown spinach. Consequently, the rate of production of these oxidative modifications and their possible role in the photoinhibitory process is unknown at this time.

On the oxidizing side of the photosystem, a number of oxidatively modified residues have been identified using tandem mass spectrometry. The Barry laboratory has been at the forefront

of this research [207, 208]. *N*-formykynurenine(NFK) is an oxidative modification of tryptophan which appears, in at least some systems,to be involved in the response to oxidative stress [209]and is a marker for high light stress in plants [207]. Conversion of tryptophan to NFK involves a double oxidation event which leads to ring opening and an expected mass change of +32 Da. The ROS species responsible for NFK formation include O_2* [210] and $^{\bullet}$OH[211], both of which have been implicated in photoinhibition (see above). A number of tryptophanyl residues oxidatively modified to NFK have been identified in PS II and the presence of some of these is directly correlated to photoinhibition. Dreaden et al. [207] presented compelling evidence that CP 43:^{365}W was modified to NFK. The presence of NFK was verified using UV-Vis spectroscopy, UV resonance Raman spectroscopy and tandem mass spectrometry. Photoinhibition experiments performed on PS II membranes indicated that the loss of oxygen evolution capability very closely tracked the appearance of increasing amounts of NFK: a 2.4 ± 0.5-fold decrease in oxygen evolution capacity and a 2.4 ± 0.8-foldincrease in NFK during photoinhibition. CP 43:^{365}W is located 17 Å from the Mn_4O_5Ca oxygen-evolving site (Fig. 11). Other tryptophanyl residues are also located in the vicinity of the metal cluster. CP43:^{359}W, CP 43:^{291}W and D2:^{328}W are all located within a 16 Å sphere surrounding the metal cluster, but were not observed to be oxidatively modified. This may indicate some specificity with regard to CP 43:^{365}W modification. Earlier, this laboratory had reported that site-directed mutations introduced at the analogous site in *Synechocystis*6803 (CP43:^{352}W) yielded mutants which did not exhibit defects in oxygen evolution but which were much more susceptible to photoinhibition[212].

Interestingly, very modest increases in the ionic strength of the buffer present during photoinhibition leads to the loss of NFK formation at CP 43:^{365}W and the appearance of a new NFK modification at D1:^{317}W[208]. This residue is also located in close proximity (14 Å) to the Mn_4O_5Ca metal cluster (Fig. 11). The authors hypothesized that ionic changes (possibly Mg^{+2}) in the thylakoid membranes occurring in response to illumination may trigger alteration in the oxidative modification pattern observed for these residues.

In our laboratory, we have also used tandem mass spectrometry to examine oxidative modifications in the vicinity of the Mn_4O_5Ca oxygen-evolving site [50]. A group of oxidized CP 43 residues (^{354}E, ^{355}T, ^{356}M and ^{357}R) which are located in close proximity (≤10 Å) to the manganese clusterwere identified to be natively oxidized in PS II membranes which had been isolated from field spinach. CP 43:^{354}E is a bidentate, first shell ligand to Mn2 and Mn3, while CP 43:^{357}R is a second sphere ligand associated with O2 and O4 of the manganese cluster [6]. While this study identifies the manganese cluster as being a probable source of ROS, it does not provide information as to its importance in ROS production in the photoinhibition process.It has been hypothesized that these four CP 43 residues may be associated with an oxygen/ROS egress channel (Fig. 11) on the oxidizing side of the photosystem [75].

UsingMALDI-TOF, tandem mass spectrometry and X-ray crystallography,Sugiura et al. [213]demonstrated that D2:^{336}H (Fig. 13) was oxidatively modified in *Thermosynechococcus*. Examination of the electron density maps from *Thermosynechococcus*[6] indicated that a significant electron density anomaly was located adjacent to D2:^{336}H in both PS II monomers (Fig. 11). This modification was consistent with the possible oxidative modification of this residue. Such modification could be the result of posttranslational modification or an artifactdue to ROS produced by the X-ray beam. To distinguish between these two possibilities, the authors isolated the D2 protein after SDS-PAGE of PS II core complexes which had never been exposed to X-rays, performed *in situ* trypsin digestion and analyzed the proteolytic fragments by mass

spectrometry. These experiments verified that D2:^{336}H was posttranslationally oxidatively modified and that about 20-30% of the D2 proteins carry this modification.

3. Some Future Directions

3.3.1 Mapping of components within assembly complexes

PS II consists of numerous subunits and cofactors which must be assembled in a precisely orchestrated sequence of molecular events[52]. This process involves the participation of assembly factors that facilitate and coordinate the sequential addition of structural subunits(and pigments/cofactors),forming transiently quasi-stable assembly complexes. These assembly complexes are usually present in very low concentrations within the photosynthetic membrane, precluding their isolation in sufficient quantities for protein crystallization. Consequently, other methods are required to examine and identify the protein-protein interactions within such assembly complexes, particularly in regard to the possible interactions of theassembly factors with each other and their interaction(s) with the structural components of the photosynthetic complexes.

The use of mass spectrometry coupled with protein crosslinking and/or protein footprinting holds great promise for identifying protein-protein interactions within assembly complexes. Such experiments in conjunction with (1) X-ray crystallographic and/or NMRstructural examination of assembly factors which have been expressed heterologously, and (2) protein modeling of the interacting domains between assembly factors and their associated structural subunits, may provide a glimpse of the structural organization of assembly complexes.In this regard the crystal and/or NMR structures of several assembly factors associated with cyanobacterial PS II are known (Psb27[25, 214], CyanoP [21, 22] and Ycf48/Hcf136 [27]) and Psb28 [215].

A first example of this approach is the examination of the association of the assembly factor Psb27 with cyanobacterial PS II [114]. Psb27 facilitates the assembly of the manganese cluster in PS II [216], participates in PS II repair [217], and had been shown to be associated with PS II complexes which partially assemble in the absence of the C-terminal D1 processing enzyme *ctp*A[218]. The interaction of Psb27 with PS II assembly intermediates has been examined in *Synechocystis* 6803 PS IIusing protein crosslinking and mass spectrometry[114]. Using the protein crosslinkers EDC (0-length) and DTSSP (12Å), these authors determined that Psb27 interacted directly with CP 43(Fig. 12A). EDC crosslinking coupled with tandem mass spectrometry identified salt bridges between Psb27:^{58}D and CP 43:^{215}K and Psb27:^{63}K and CP 43:^{321}D. Interestingly, the distance between CP43: ^{215}K and CP43:^{321}D in mature PS II (32.8Å) is greater than the distance between Psb27:^{58}D and Psb27:^{63}K (11.3Å -19.8Å) in the NMR structures of Psb27 [25, 214]. This indicates that either Psb27 or PS II undergoes a 12.5-21.5Å conformational change when associated in an assembly complex or that two different locations are present for Psb27 binding to CP 43, one adjacent to CP43: ^{215}K and the other adjacent to CP43:^{321}D. These possibilities cannot be distinguished at this time.

These investigators also used site-specific labeling techniques of carboxylates to further refine their analysis of the interaction of Psb27 within the PS II assembly complex [96]. They found that the interacting domain of CP 43 with Psb27 included the residues CP 43:^{367}E, ^{376}E, ^{378}E, and ^{383}E (Fig. 12B). Binding of Psb27 to this domain may prevent binding of PsbO and PsbV to this assembly complex.

Although these studies are quite promising several caveats must be considered in these types of experiments. Firstis the assumption that the molecular organization of the structural protein subunits in an assembly complex approximates that which is observed for these subunits in the mature membrane protein complex being modeled.This may or may not be the case. Similarly, the bound structure of an assembly factor may be different from its solution structure. A careful analysis of crosslinked/modified species involving ***only***the structural subunits and ***only*** the assembly factor in control experiments may reveal structural alterations in the subunit/assembly factor which are specific for assembly complexes, only.

3.3.2*In vivo*and *in organello*protein crosslinking

Clearly, an ultimate goal of structural biology is understanding the *in vivo* structure of membrane protein complexes. As noted in the introduction, this is difficult to accomplish using only the traditional tools of X-ray crystallography. *In vivo* and *in organello* protein crosslinking promise to provide critical supplementary information bearing on subunit topology and makeup, functional architecture and protein complex interactions [219]. A number of protein crosslinkers are hydrophobic and consequently have the ability to cross biological membranes.These can crosslink protein components *in vivo*or *in organello*. These include formaldehyde (2 Å spacer), the homobifunctional crosslinkerDTSP, the heterobifunctional photoactivatablecrosslinkers succinimidyl 4,4'-azipentanoate (NHS-diazirine,3.9 Å spacer arm) and succinimidyl 2-([4,4'-azipentanamido]ethyl)-1,3'-dithiopropionate (NHS-SS-diazirine, 13.5 Å spacer arm), and others.*In vivo* crosslinking appears to be particularly attractive in the identification of transient protein-protein interactions occurring in photosynthetic membranes upon changing environmental conditions. These include state transitions, high light or temperature photoinhibition, diurnal cycling, anaerobiosis, nutrient limitation, etc. All of these conditions have been reported to influence the photosynthetic apparatus; however, elucidation of the molecular mechanisms involved is hampered by the necessity to isolate photosynthetic membranes prior to the analysis of the photosynthetic complexes. It is likely that many, if not most, transient protein-protein interactions may not survive this isolation procedure. Additionally, it must be pointed out that our current knowledge of the structural components associated with the photosynthetic membrane protein complexes is based almost entirely on detergent-isolated complexes. It is formally possible that structural components of these complexes may be present under native conditions but are lost during the crystallization process. This is known to occur during isolation and crystallization of cyanobacterial PS II. The CyanoQ component is lost [17, 162] and does not appear in the current crystal structures [6, 7]. Possible reasons for the loss of subunits include release at the detergent concentrations used during solubilization of the photosynthetic membrane, loss during purification, the ionic make-up of the crystallization liquor (usually very different from*in vivo* conditions), sensitivity to required crystallization conditions (pH, metal additives, amphiphilic additives, etc.), steric hindrance either within detergent micelles or in the crystal matrix, etc.

In either application the use of *in vivo/in organello* protein crosslinking “freezes” the protein-protein interaction so that the association of the interacting partners survives the isolation and subsequent analysis steps. In this regard it should be noted that *in vivo* protein-DNA crosslinking with formaldehyde is a well established procedure in the examination of chromatin structure[220, 221]. Interestingly, *in vitro,*even at very high concentration of bovine serum albumin (50 mg/ml, which approximates *in vivo* protein concentrations) BSA was not observed

to be crosslinked artifactually to DNAwith formaldehyde[220]. This observation supports the hypothesis that, in large measure, formaldehyde identifies specific protein-DNA interactions. This may also indicate low levels of artifactual protein-protein crosslinking *in vivo*. One recent example of the use of *in vivo*formaldehyde crosslinking is examination of the association of the Rubisco Accumulation Factor 1 (RAF1) with the large subunit of Rubisco[222]. RAF1 is required for Rubisco accumulation. In the absence of RAF1, Rubisco transcription and translation are not affected but Rubisco fails to accumulate, which suggests that RAF1 is a chaperonin for Rubisco. After *in vivo* crosslinking followed by BN-gel electrophoresis, a 750 kDa complex was identified which contained both RAF1 and the large subunit of Rubisco. After immunoprecipitation with an anti-RAF1 antibody, SDS-PAGE analysis identified a specific crosslinked product containing the large subunit of Rubisco and RAF1. Mass spectrometry could be used to identify other proteins possibly present in the 750 kDa native complex and possibly the site of interaction between the large subunit of Rubisco and RAF1.

Another possible approach for *in vivo* protein crosslinking is the metabolic incorporation of non-canonical amino acid analogues which act as photoactivatable protein crosslinkers. Two reagents, L-Photo-leucine and L-Photo-methionine are commercially available (Pierce Chemical Co.). Both of these reagents contain diazirine functional groups which are activated by exposure to 365 nm ultraviolet light. Optimally, metabolic incorporation requiresthe use of leucine or methionineauxotrophs which, at this time, would appear to limit their use to cyanobacterialor other bacterial systems.No verified leucine or methionine auxotrophs have been isolated in *Chlamydomonas* (*Chlamydomonas* Sourcebook).In this regard, methionine auxotrophs have been reported for *Synechococcus* sp. 6301 [223], *Anabaena variabilis*[224]and *Synechococcus* 7942 [225],while a leucine auxotroph has been reported for *Synechocystis* 6803 [226]. This latter mutant was the result of an insertion in the *sod*B gene (encoding superoxide dismutase) that induced a polar effect on the downstream *leu*B gene.

It should be noted that in higher plants, a number of herbicides inhibit ketol-acid reductoisomerase (acetohydroxyacid synthase, EC 1.1.1.86), which is the second common step in branched chain amino acid biosynthesis. These inhibitors include N-isopropyl oxalylhydroxamate (IpOHA), 2-dimethylphosphinoyl-2-hydroxyacetic acid (HOE 704) and CPCA (1,1-cyclopropanedicarboxylic acid). In *Arabidopsis*, 10 ppm HOE 704 completely inhibits growth. Interestingly, the effect of the herbicide can be largely reversed by supplementation of the growth medium with 0.5 mM each of valine, leucine and isoleucine[227, 228]. This observation raises the intriguing possibility that L-photo-leucine could be incorporated into higher plantsin the presence of these inhibitors. Given that the branched chain amino acid biosynthetic pathway appears to be highly conserved (all of these inhibitors also inhibit the *E. coli* enzyme), incorporation of L-Photo-leucineinto *Chlamydomonas*, cyanobacteria and other plant model systems by this proposed method may also be possible.

4. Conclusion

The use of tandem mass spectrometry in combination with protein modification methodologiesto examine PS II is still in its infancy. The explosion of studies using these techniques over the last five years indicates that these methods will become increasingly important in the examination of PS II structure and function. Even at this early stage, substantial contributions have been made in the understanding of subunit-subunit interactions within the phycobilisome antennae, the structure and mechanism of cyanobacterial OCP, the locations of the important extrinsic subunits

(CyanoQ, PsbP and PsbQ), the identification of buried water and possibly, oxygen/ROS pathways, and the identification of posttranslational modifications within the photosystem. Particularly promising is the possibility that exploitation of *in vivo* chemical modification methodologies will allow the identification and structural examination of assembly/repair complexes and other transient complexes present during environmental changes.We look forward to additional findings on these topics and others that will undoubtedly be forthcoming in the near future.

Acknowledgments:

This work was supported by the Division of Chemical Sciences, Geosciences, and Biosciences, Office ofBasic Energy Sciences of the U.S. Department of Energy through grant DE-FG02-98ER20310 to T.M.Band L.K.F. Special thanks are given to Annette Hebert for her critical reading of the manuscript.

Figure Legends

Figure 1. PS II. Shown is the 1.9 Å crystal structure of the PS II dimer from the thermophilic cyanobacterium *Thermosynechococcus vulcanus*[6]. A. View of the complex from within the plane of the membrane, B. view of the lumenal face of the complex. D1, yellow; D2, pale yellow; PsbI, orange; PsbE, red;CP 43, dark green; CP 47, light green;PsbO, blue; PsbU, pale blue; PsbV,purple; all other subunits are illustrated in grey.

Figure 2. High Quality Tandem Mass Spectrometry Result for the Tryptic Peptide PsbO:^{81}L-^{101}K. Upper Panel, mass spectrum of peptide.Within the peptide sequence shown, red letters indicate identification of residues in both consecutive y- and b-ions; green letters, residues identified in consecutive y-ions; blue letters, residues identified in consecutive b-ions, and black letters, residues not identified.This precursor peptide was observed as a triply charged ionand had a predicted mass of 2300.1180 Da and an observed mass of 2300.1139 Da,with a consequentmass accuracy of 1.7 ppm and a p-value of 10^{-21}. Lower Panel, table of predicted product ions from this amino acid sequence of this peptide.Ions which were detected are shown in red. A continuous y-ion series was observed from y3 to y19 and a continuous b-ion series was observed from b4 to b20. y* and b*, neutral loss of ammonia; y' and b', neutral loss of water.

Figure 3. Peptide Identification at Various p-Values for the Tryptic Peptide PsbO:^{6}L-^{14}K. Shown is the mass spectrum obtained for the this peptide at various p-values. Three p-values are illustrated, $p = 10^{-8}$, upper panel; $p = 10^{-4}$, middle panel; and $p = 10^{-2}$, lower panel. As the p-values decrease, the number of predicted y- and b-ions identified in the data increases, as does the reliability of the peptide identification. Within the peptide sequence shown above each panel, red letters indicate identification of residues identified in both consecutive y- and b-ions; green letters, residues identified in consecutive y-ions; blue letters, residues identified in consecutive b-ions, and black letters, residues not identified. Below the mass spectrum in each panel is the table of predicted product ions from the amino acid sequence of this peptide. Ions which were detected are shown in red.

Figure 4. Structures of Some Reagents Recently Used for PS II Modification and Analysis by Tandem Mass Spectrometry. In parentheses are common names and, in the case of crosslinking reagents, the maximum distance between crosslinked residues. EDC can be used either as a protein crosslinker or, in the presence of excess glycine methyl ester or glycine ethyl ester, a site-specific labeling reagent.

Figure 5. Partial Interaction Map of Phycobilisome Subunits. Only the crosslinking interactions exhibiting low p-values from [119]are illustrated; for a more complete map the reader should consult the original paper. Blue, phycocyanin subunits; cyan, allophycocyanin subunits.Individual crosslinked products are labeled and indicated by lines.

Figure 6. InteractionMaps of PhycobilosomeSubunitswith PS Iand PS II.
A. Phycobilisome-PS I interactions illustrating the crosslinked products observed between their subunits [115]. B. Phycobilisome-PS II interactions illustrating the crosslinked products observed between their subunits. Dark green,PS I subunits; pale green, PS II subunits;blue,

phycocyanin subunits;cyan, allophycocyanin subunits. Individual crosslinked products are labeled and indicated by lines.

Figure 7. OCP Interactions with Allophycocyanin and Light-Induced OCP Conformational Changes.A. Interaction map of OCP with allophycocyanin.Cyan, allophycocyanin subunits;orange, OCP; blue, phycocyanin subunits, which were observed to be crosslinked to each other but not to allophycocyanin of the OCP[118]. Individual crosslinked products are indicated by lines and are labeled. B. Observed conformational changes upon conversion of OCP^o to OCP^r. Red, increased chemical labeling of carboxylates in the OCP^r state; pink, decreased chemical labeling in the OCP^r state; blue, decreased radiolytic modification in the OCP^r state; light-blue, increased radiolytic modification in the OCP^r state[97, 157].

Figure 8.Interactions of CyanoQ within Cyanobacterial PS II. A. Interaction map of CyanoQ with other PS II subunits. Green, PsbB; white, PsbO and CyanoQ [117]. Individual crosslinked products are indicated by lines and are labeled. B. Proposed structure of the symmetrical CyanoQ-CyanoQ dimer with one subunit shown in pink and the other in light green. Residues shown as spheres are involved in crosslinking; red residues and green residues participate in inter-PsbQ subunit crosslinked products and the distances between these residues are shown. The other residues shown as spheres are involved in crosslinking PsbQ to PsbO and PsbB.

Figure 9.Interactions of PsbP and PsbQ within Higher Plant PS II.A. Interaction map of PsbP and PsbQ with other PS II subunits. Green, CP 26, PsbE and PsbR;white, PsbP and PsbQ [78, 116, 167]. Individual crosslinked products are indicated by lines and are labeled. For clarity, the nine independent crosslinked products between the N- and C-terminal domains within PsbP have been omitted [78]. B. Proposed structural interaction between PsbP (pale-green) and PsbQ (pale-blue). The distances between the crosslinked residues are labeled. C. Proposed structure of the higher plant PsbQ-PsbQ dimer with one subunit shown in light blue and the other in blue. The distances between the inter-PsbQcrosslinked residues are labeled.

Figure 10.Identification of Putative Water Channels and Oxygen Egress Pathways in Higher Plant PS II. The oxidatively modified residues aremapped onto the 1.9 Å cyanobacterial crystal structure[6]. A. Residues associated with a putative water channel. B. Residues associated with aputative oxygen or ROS egress pathway. Pink, CP 47;light brown, D2; pale yellow, D1; pale green, CP 43; blue, PsbO. Modified residues are shown as spheres in darker shades. It should be noted that the modified residues ^{363}F (in A.) and ^{355}T (in B.) are not visible in these views.

Figure 11. Natively Oxidized Residues in PS II. Natively oxidized residues are mapped onto the 1.9 Å cyanobacterial crystal structure [6] and shown as spheres. The PS II cofactors are shown as sticks and are labeled, the proteins (yellow, D1; brown, D2; and green, CP43) are shown in the background. D2:^{336}H was identified in *Thermosynechococcus*[213]; all other residues were identified in higher plants[75, 77, 207, 208].

Figure 12. Interaction of CP 43 with the Assembly Factor Psb27.A. Interaction map of CP43 with Psb27 [114]. Green, CP43;white, Psb27. Individual crosslinked products are indicated

by lines and are labeled. B. Chemical footprinting of the CP 43-Psb27 interaction. Green spheres,CP 43 residues labeled in the absence of Psb27. The CP43 residues identified as being crosslinked to Psb27:^{216}K and ^{321}D are shown in blue and red spheres, respectively[96].

5. REFERENCES

[1] J. Deisenhofer, O. Epp, K. Miki, R. Huber, H. Michel, X-ray structure analysis of a membrane protein complex electron density map at 3 angstrom resolution and a model of the chromophores of the photosynthetic reaction center from *Rhodopseudomonas viridis*, J Mol Biol, 180 (1984) 385-398.

[2] J. Deisenhofer, O. Epp, K. Miki , R. Huber, H. Michel, Structure of the protein subunits in the photosynthetic reaction center of *Rhodopseudomonas viridis* at 3 Å resolution, Nature, 318 (1985) 618-623.

[3] A. Zouni, H.-T. Witt, J. Kern, P. Fromme, N. Krauss, W. Saenger, P. Orth, Crystal structure of Photosystem II from *Synechococcus elongatus* at 3.8 Å resolution, Nature, 409 (2001) 739-743.

[4] J. Biesiadka, B. Loll, J. Kern, K.-D. Irrgang, A. Zouni, Crystal structure of cyanobacterial Photosystem II at 3.2 A resolution: a closer look at the Mn-cluster, Phys Chem Chem Phys, 6 (2004) 4733-4736.

[5] B. Loll, N. Kern, W. Saenger, A. Zouni, J. Biesiadka, Towards complete cofactor arrangement in the 3.0 Å resolution structure of Photosystem II, Nature, 438 (2006) 1040-1044.

[6] Y. Umena, K. Kawakami, J.-R. Shen, N. Kamiya, Crystal structure of oxygen-evolving Photosystem II at a resolution of 1.9 Å, Nature, 473 (2011) 55-60.

[7] M. Suga, F. Akita, K. Hirata, G. Ueno, H. Murakami, Y. Nakajima, T. Shimizu, K. Yamashita, M. Yamamoto, H. Ago, J.R. Shen, Native structure of Photosystem II at 1.95 angstrom resolution viewed by femtosecond X-ray pulses, Nature, 517 (2015) 99-103.

[8] P. Jordan, P. Fromme, H.T. Witt, O. Klukas, W. Saenger, N. Krauss, Three-dimensional structure of cyanobacterial Photosystem I at 2.5 A resolution, Nature, 411 (2001) 909-917.

[9] A. Amunts, H. Toporik, A. Borovikova, N. Nelson, Structure determination and improved model of plant Photosystem I, J Biol Chem, 285 (2010) 3478-3486.

[10] G. Kurisu, H. Zhang, J.L. Smith, W.A. Cramer, Structure of the cytochrome b_6f complex of oxygenic photosynthesis: tuning the cavity, Science, 302 (2003) 1009-1014.

[11] D. Stroebel, Y. Choquet, J.L. Popot, D. Picot, An atypical haem in the cytochrome b_6f complex, Nature, 426 (2003) 413-418.

[12] J.P. Abrahams, A.G.W. Leslie, R. Lutter, J.E. Walker, Structure at 2.8 Å resolution of F_1-ATPase from bovine heart mitochondria, Nature, 370 (1994) 621-628.

[13] Z.F. Liu, H.C. Yan, K.B. Wang, T.Y. Kuang, J.P. Zhang, L.L. Gui, X.M. An, W.R. Chang, Crystal structure of spinach major light-harvesting complex at 2.72 angstrom resolution, Nature, 428 (2004) 287-292.

[14] R.J. Cogdell, A.A. Freer, N.W. Isaacs, A.M. Hawthornthwaite-Lawless, G. Mcdermott, M.Z. Papiz, S.M. Prince, Integral Membrane peripheral light harvesting complex from *Rhodopseudomonas acidophila* strain 10050, J Mol Biol, 268 (1997) 412-423.

[15] M. Duerring, G.B. Schmidt, R. Huber, Isolation, crystallization, crystal structure analysis and refinement of constitutive C-phycocyanin from the chromatically adapting cyanobacterium *Fremyella diplosiphon* at 1.66 Å resolution, J Mol Biol, 217 (1991) 577-592.

[16] A. Marx, N. Adir, Allophycocyanin and phycocyanin crystal structures reveal facets of phycobilisome assembly, Biochim Biophys Acta, 1827 (2013) 311-318.
[17] F. Michoux, M. Boehm, J. Bialek, K. Takasaka, K. Maghlaoui, J. Barber, J.W. Murray, P.J. Nixon, Crystal structure of CyanoQ from the thermophilic cyanobacterium *Thermosynechococcus elongatus* and detection in isolated Photosystem II complexes, Photosyn Res, 122 (2014) 57-67.
[18] V. Calderone, M. Trabucco, A. Vujičić, R. Battistutta, G.M. Giacometti, F. Andreucci, R. Barbato, G. Zanotti, Crystal structure of the PsbQ protein of Photosystem II from higher plants, EMBO Rep, 4 (2003) 900-905.
[19] J.A. Hermoso, M. Balsera, J. De las Rivas, J. Arellano, Crystal structure of the 16 kDa protein from higher plants, PDB Accession 1VYK, (2004).
[20] M. Balsera, J.B. Arellano, J.L. Revuelta, J. De Las Rivas, J.A. Hermoso, A 1.49 Å resolution crystal structure of PsbQ from Photosystem II of *Spinacia oleracea* reveals a PPII structure in the N-terminal region, J Mol Biol, 350 (2005) 1051-1058.
[21] S.A. Jackson, M.G. Hinds, J.J. Eaton-Rye, Solution structure of CyanoP from *Synechocystis* sp. PCC 6803: New insights on the structural basis for functional specialization amongst PsbP family proteins, Biochim Biophys Acta, 1817 (2012) 1331-1338.
[22] F. Michoux, K. Takasaka, M. Boehm, P.J. Nixon, J.W. Murray, Structure of CyanoP at 2.8 Å: implications for the evolution and function of the PsbP subunit of Photosystem II, Biochemistry, 49 (2010) 7411-7413.
[23] K. Ifuku, T. Nakatsu, H. Kato, F. Sato, Crystal structure of the PsbP protein of Photosystem II from *Nicotiana tabacum*, EMBO Rep, 5 (2004) 362-367.
[24] P. Cao, Y. Xie, M. Li, X. Pan, H. Zhang, X. Zhao, X. Su, T. Cheng, W. Chang, Crystal structure analysis of extrinsic PsbP protein of Photosystem II reveals a manganese-induced conformational change, Mol Plant, 8 (2015) 664-666.
[25] K.U. Cormann, J.A. Bangert, M. Ikeuchi, M. Rogner, R. Stoll, M.M. Nowaczyk, Structure of Psb27 in solution: implications for transient binding to Photosystem II during biogenesis and repair, Biochemistrty, 48 (2009) 8768-8770.
[26] Y. Yang, T.A. Ramelot, J.R. Cort, D. Wang, C. Ciccosanti, K. Hamilton, R. Nair, B. Rost, T.B. Acton, R. Xiao, J.K. Everett, G.T. Montelione, M.A. Kennedy, Solution NMR structure of Photosystem II reaction center protein Psb28 from *Synechocystis* sp. Strain PCC 6803, Proteins, 79 (2011) 340-344.
[27] F. Michoux, K. Takasaka, P.J. Nixon, J.W. Murray, Crystal structure of Ycf48 from *Thermosynechoccus elongatus*, Protein Data Bank, (2011).
[28] R. Nagao, M. Suga, A. Niikura, A. Okumura, F.H.M. Koua, S. T., T. Tomo, I. Enami, J.-R. Shen, Crystal structure of Psb31, a novel extrinsic protein of Photosystem II from a marine centric diatom and implications for its binding and function, Biochemistry, 52 (2013) 6646-6652.
[29] J. Nield, E.V. Orlova, E.P. Morris, B. Gowen, M. van Heel, J. Barber, 3D map of the plant Photosystem II supercomplex obtained by cryoelectron microscopy and single particle analysis, Nat Struct Biol, 7 (2000) 44-47.
[30] J. Nield, J. Barber, Refinement of the structural model for the Photosystem II supercomplex of higher plants., Biochim Biophys Acta, 1757 (2006) 353-361.
[31] S. Caffarri, R. Kouril, S. Kereiche, E.J. Boekema, R. Croce, Functional architecture of higher plant Photosystem II supercomplexes, EMBO J, 28 (2009) 3052-3063.

[32] S. Barera, C. Pagliano, T. Pape, G. Saracco, J. Barber, Characterization of PSII–LHCII supercomplexes isolated from pea thylakoid membrane by one-step treatment with α- and β-dodecyl-D-maltoside, Philos Trans R Soc Lond B Biol, 367 (2012) 3389-3399.
[33] B. Drop, M. Webber-Birungi, S.K.N. Yadav, A. Filipowicz-Szymanska, F. Fusetti, E.J. Boekema, R. Croce, Light-harvesting complex II (LHCII) and its supramolecular organization in C*hlamydomonas reinhardtii*, Biochim Biophys Acta, 1837 (2014) 63-72.
[34] P. Galka, S. Santabarbara, T.T.H. Khuong, H. Degand, P. Morsomme, R.C. Jennings, E.J. Boekema, S. Caffarri, Functional analyses of the plant Photosystem I–Light-Harvesting Complex II Supercomplex reveal that Light-Harvesting Complex II loosely bound to Photosystem II Is a very efficient antenna for Photosystem I in state II, Plant Cell, 24 (2012) 2963-2978.
[35] A.A. Arteni, L.-N. Liu, T.J. Aartsma, Y.-Z. Zhang, B.-C. Zhou, E.J. Boekema, Structure and organization of phycobilisomes on membranes of the red alga *Porphyridium cruentum*, Photosyn Res, 95 (2008) 169-174.
[36] A. Busch, J. Nield, M. Hippler, The composition and structure of Photosystem I-associated antenna from *Cyanidioschyzon merolae*, Plant J, 62 (2010) 886-897.
[37] M. Watanabe, D.A. Semchonokc, M.T. Webber-Birungic, S. Ehira, K. Kondo, R. Narikawa, M. Ohmori, E.J. Boekema, M. Ikeuch, Attachment of phycobilisomes in an antenna–Photosystem I supercomplex of cyanobacteria, Proc Natl Acad Sci (USA), 111 (2014) 2512-2517.
[38] H. Kirchoff, S. Lenhert, C. Buchel, H. Chi, J. Nield, Probing the organization of Photosystem II in photosynthetic membranes by atomic force microscopy†, Biochemistry, 47 (2008) 431-449.
[39] K. Sznee, J.P. Dekker, R.T. Dame, H. van Roon, G.J.L. Wuite, R.N. Frese, Jumping mode atomic force microscopy on grana membranes from spinach, J Biol Chem, 286 (2011) 39164-39171.
[40] L.-N. Liu, S. Scheuring, Investigation of photosynthetic membrane structure using atomic force microscopy, Trends Plant Sci, 18 (2013) 277-286.
[41] M. Sharon, How far can we go with structural mass spectrometry of protein complexes?, J Amer Soc Mass Spec, 21 (2010) 487-500.
[42] J. Rappsilber, The beginning of a beautiful friendship: Cross-linking/mass spectrometry and modelling of proteins and multi-protein complexes, J Struct Biol, 173 (2011) 530-540.
[43] L. Walzthoeni, A., F. Stengel, R. Abersold, Mass spectrometry supported determination of protein complex structure, Curr Opin Struct Biol, 23 (2013) 252-260.
[44] N.P. Barrera, C.V. Robinson, Advances in the mass spectrometry of membrane proteins: from individual proteins to intact complexes, Ann Rev Biochem, 80 (2010) 247-271.
[45] A. Gabdulkhakov, M. Broser, A. Guskov, J. Kern, C. Glockner, F. Muh, W. Saenger, A. Zouni, Structural basis of cyanobacterial Photosystem II Inhibition by the herbicide terbutryn, J Biol Chem, 286 (2011) 15964-15972.
[46] S.S. Hasan, E. Yamashita, S. Baniulis, W.A. Cramer, Quinone-dependent proton transfer pathways in the photosynthetic cytochrome b_6/f complex, Proc Natl Acad Sci (USA), 110 (2013) 4297-4302.
[47] C.W. Cady, R.H. Crabtree, G.W. Brudvig, Functional Models for the oxygen-evolving complex of Photosystem II, Coord Chem Rev, 252 (2008) 444-455.
[48] J.R. Shen, The Structure of Photosystem II and the mechanism of water oxidation in photosynthesis, Ann Rev Biochem, 66 (2015) 23-48.

[49] T.M. Bricker, L.K. Frankel, Auxiliary functions of the PsbO, PsbP and PsbQ proteins of higher plant Photosystem II: A critical analysis, J Photochem Photobiol B: Biol, 104 (2011) 165-178.
[50] T.M. Bricker, J.L. Roose, R.D. Fagerlund, L.K. Frankel, J.J. Eaton–Rye, The extrinsic proteins of Photosystem II, Biochim Biophys Acta, 1817 (2012) 121-142.
[51] T.M. Bricker, L.K. Frankel, The structure and function of the 33 kDa extrinsic protein of Photosystem II. A critical review, Photosyn Res, 56 (1998) 157-173.
[52] P.J. Nixon, F. Michoux, J. Yu, M. Boehm, J. Komenda, Recent advances in understanding the assembly and repair of Photosystem II, Ann Bot, 106 (2010) 1-16.
[53] P. Pospíšil, A. Arató, A. Krieger-Liszkay, A.W. Rutherford, Hydroxyl radical generation by Photosystem II, Biochemistry, 43 (2004) 6783-6792.
[54] P. Pospíšil, Production of reactive oxygen species by Photosystem II, Biochim Biophys Acta, 1787 (2009) 1151-1160.
[55] N. Nelson, C.F. Yocum, Structure and function of Photosystems I and II, Ann Rev Plant Biol, 57 (2006) 521-565.
[56] G. Renger, T. Renger, Photosystem II:The machinery of photosynthetic water splitting, Photosyn Res, 98 (2008) 53-80.
[57] G. Renger, Light induced oxidative water splitting in photosynthesis: Energetics, kinetics and mechanism, Photochem Photobiol B: Biology, 104 (2011) 35-43.
[58] D.J. Vinyard, G.M. Ananyev, G.C. Dismukes, Photosystem II: The reaction center of oxygenic photosynthesis, Annu Rev Biochem, 82 (2013) 577-606.
[59] B.T. Chait, Mass spectrometry: Bottom-up or top-down, Science, 314 (2006) 65-66.
[60] B.A. Garcia, What does the future hold for top-down mass spectrometry?, J Am Soc Mass Spectrom, 21 (2010) 193-202.
[61] J. Marcoux, S. Cianferani, Towards integrative structural mass spectrometry: Benefits from hybrid approaches, Methods, in press (2015).
[62] A. El-Aneed, A. Cohen, J. Banoub, Mass spectrometry, review of the basics: Electrospray, MALDI, and commonly used mass analyzers, App Spect Rev, 44 (2009) 210-230.
[63] B. Domon, R. Aebersold, Mass spectrometry and protein analysis, Science, 312 (2006) 212-217.
[64] X. Han, A. Aslanian, J.R. Yates III, Mass spectrometry for proteomics, Curr Opin Chem Biol, 12 (2008) 483-490.
[65] R.A. Zubarev, A. Makarov, Orbitrap mass spectrometry, Anal Chem, 85 (2013) 5288-5296.
[66] J.K. Eng, A.L. McCormack, I. Yates, J.R., An approach to correlate tandem mass spectral data of peptides with amino acid sequences in a protein database, J Am Soc Mass Spectrom, 5 (1994) 976-989.
[67] D.N. Perkins, D.J.C. Pappin, D.M. Creasy, J.S. Cottrell, Probability-based protein identification by searching sequence database using mass spectrometry data, Electrophoresis, 20 (1999) 3551–3567.
[68] S. Peri, H. Steen, A. Pandey, GPMAW - a software tool for analyzing proteins and peptides, TIBS, 26 (2001) 687-689.
[69] H. Xu, M.A. Freitas, A mass accuracy sensitive probability based scoring algorithm for database searching of tandem mass spectrometry data, BMC Bioinform, 8 (2007) 133-137.
[70] H. Xu, M.A. Freitas, MassMatrix: A database search program for rapid characterization of proteins and peptides from tandem mass spectrometry data, Proteomics, 9 (2009) 1548-1555.

[71] O. Oliver Rinner, J. Jan Seebacher, T. Thomas Walzthoeni, L.N. Lukas N Mueller, Martin Beck, M., A. Alexander Schmidt, M. Markus Mueller, R. Ruedi Aebersold, Identification of cross-linked peptides from large sequence databases, Nat Meth, 5 (2008) 315-318.
[72] B. Yang, Y.-J. Wu, M. Zhu, S.-B. Fan, J. Lin, K. Zhang, S. Li, H. Chi, Y.-X. Li, H.-F. Chen, S.-K. Luo, Y.-H. Ding, L.-H. Wang, Z. Hao, L.-Y. Xiu, S. Chen, K. Ye, S.-M. He, M.-Q. Dong, Identification of crosslinked peptides from complex samples, Nat. Meth., 9 (2012) 904-906.
[73] J. Kosinski, A. von Appen, A. Ori, K. Karius, C.W. Müller, M. Martin Beck, Xlink Analyzer: Software for analysis and visualization of cross-linking data in the context of three-dimensional structures, J Struct Biol, 189 (2015) 177-183.
[74] P. Kaur, J.G. Kiselar, M.R. Chance, Integrated algorithms for high-throughput examination of covalently labeled biomolecules by structural mass spectrometry, Anal Chem, 81 (2009) 8141-8149.
[75] L.K. Frankel, L. Sallans, P.A. Limbach, T.M. Bricker, Identification of oxidized amino acid residues in the vicinity of the Mn_4CaO_5 cluster of Photosystem II: Implications for the identification of oxygen channels within the photosystem, Biochemistry, 51 (2012) 6371-6377.
[76] L.K. Frankel, L. Sallans, H. Bellamy, J.S. Goettert, P.A. Limbach, T.M. Bricker, Radiolytic mapping of solvent contact surfaces in Photosystem II of higher plants: experimental identification of putative water channels within the photosystem, J Biol Chem, 288 (2013) 23565-23572.
[77] L.K. Frankel, L. Sallans, P.A. Limbach, T.M. Bricker, Oxidized amino acid residues in the vicinity of Q_A and $Pheo_{D1}$ of the Photosystem II reaction center: Putative generation sites of reducing-side reactive oxygen species, Plos One, 8 (2013) e58042.
[78] M.P. Mummadisetti, L.K. Frankel, H. Bellamy, L. Sallans, J.S. Goettert, M. Brylinski, P.A. Limbach, T.M. Bricker, Use of protein cross-linking and radiolytic footprinting to elucidate PsbP and PsbQ interactions within higher plant Photosystem II, Proc Natl Acad Sci (USA), 111 (2014) 16178-16183.
[79] L. Käll, J.D. Storey, M.J. MacCoss, W.S. Nobel, Assigning significance to peptides identified by tandem mass spectrometry using decoy databases, J Prot Res, 7 (2008) 29-34.
[80] H. Xu, M.A. Freitas, Monte Carlo simulation-based algorithums for analysis of shotgun proteomics data, J Prot Res, 7 (2008) 2605-2615.
[81] J.E. Elias, S.P. Gygi, Target-decoy search Strategy for mass spectrometry-based proteomics, Meth Mol Biol, 604 (2010) 55-71.
[82] W.X. Schulze, B. Usadel, Quantitation in mass-spectrometry-based proteomics, Annu Rev Plant Biol, 61 (2010) 491-516.
[83] M. Bantscheff, S. Lemeer, M.M. Savitski, B. Kuster, Quantitative mass spectrometry in proteomics: critical review update from 2007 to the present, Anal Bioanal Chem, 404 (2012) 939-965.
[84] R. Fristedt, A.V. Vener, High light induced disassembly of Photosystem II supercomplexes in arabidopsis requires STN7-dependent phosphorylation of CP29, Plos One, 6 (2011) e24565.
[85] I. Samola, A. Shapiguzov, B. Ingelsson, G. Fucile, M. Crèvecoeur, A.V. Vener, J.-D. Rochaix, M. Goldschmidt-Clermont, Identification of a Photosystem II phosphatase involved in light acclimation in arabidopsis, Plant Cell, 24 (2012) 2596-2609.
[86] H. Xue, R. Tokutsu, S.V. Verena Bergner, M. Scholz, J. Minagawa, M. Hippler, PSBR is required for efficient binding of LHCSR3 to Photosystem II - light-harvesting supercomplexes in *Chlamydomonas reinhardtii*, Plant Physiol, 167 (2015) 1566-1578.

[87] V.L. Mendoza, R.W. Vachet, Probing protein structure by amino acid-specific covalent labeling and mass spectrometry, Mass Spectrom Rev, 28 (2009) 785-815.
[88] L.K. Frankel, T.M. Bricker, Interaction of CPa-1 with the manganese-stabilizing protein of Photosystem II: Identification of domains on CPa-1 which are shielded from N-hydroxysuccinimide biotinylation by the manganese-stabilizing protein, Biochemistry, 31 (1992) 11059-11063.
[89] W. Odom, T.M. Bricker, Interaction of CPa-1 with the manganese-stabilizing protein of Photosystem II: Identification of domains cross-linked by 1-ethyl-3-[3-(dimethylamino) propyl]carbodiimide, Biochemistry, 31 (1992) 5616-5620.
[90] H. Ohta, N. Yoshida, M. Sano, M. Hirano, K. Nakazato, I. Enami, Evidence for electrostatic interaction of the loop A on CP 47 with the extrinsic 33 kDa protein., in: P. Mathis (Ed.) Photosynthesis: from Light to Biosphere, Kluwer Academic Publishers, 1995, pp. 361-364.
[91] L.K. Frankel, J.A. Cruz, T.M. Bricker, The role of carboxylic acid residues on the manganese-stabilizing protein in its binding to Photosystem II, Biochemistry, 38 (1999) 14271-14278.
[92] T.M. Bricker , L.K. Frankel, Carboxylate groups on the manganese-stabilizing protein are required for efficient binding of the 24 kDa extrinsic protein to Photosystem II., Biochemistry, 42 (2003) 2056-2061.
[93] A. Tohri, N. Dohmae, T. Suzuki, H. Ohta, Y. Inoue, I. Enami, Identification of domains on the extrinsic 23 kDa protein possibly involved in electrostatic interaction with the extrinsic 33 kDa protein in spinach Photosystem II, Eur J Biochem, 271 (2004) 962-971.
[94] J. Meades, G.D., A. McLachlan, L. Sallans, P.A. Limbach, T.M. Bricker, Association of the 17 kDa extrinsic protein with Photosystem II in higher plants, Biochemistry, 44 (2005) 15216-15221.
[95] T. Nishimura, C. Uno, K. Ido, R. Nagao, T. Noguchi, F. Sato, K. Ifuku, Identification of the basic amino acid residues on the PsbP protein involved in the electrostatic interaction with Photosystem II, Biochim Biophys Acta, 1837 (2014) 1447-1453.
[96] H. Liu, J. Chen, R.Y.-C. Huang, D. Weisz, M.L. Gross, H.B. Pakrasi, Mass Spectrometry-based footprinting reveals structural dynamics of Loop E of the chlorophyll-binding protein CP43 during Photosystem II assembly in the cyanobacterium *Synechocystis* 6803, J Biol Chem, 288 (2013) 14212-14220.
[97] H. Liu, H. Zhang, J.D. Kinga, N.R. Wolf, M. Prado, M.L. Gross, R.E. Blankenship, Mass spectrometry footprinting reveals the structural rearrangements of cyanobacterial orange carotenoid protein upon light activation, Biochim Biophys Acta, 1837 (2014) 1955-1963.
[98] K. Takamoto, M.R. Chance, Radiolytic protein footprinting with mass spectrometry to probe the structure of macromolecular complexes, Ann Rev Biophys Biomol Struct, 35 (2006) 251-276.
[99] T.E. Angel, S. Gupta, B. Jastrzebska, K. Palczewski, M. Chance, Structural waters define a functional channel mediating activation of the GPCR, rhodopsin, Proc Natl Acad Sci (USA), 106 (2009) 14367-14372.
[100] J.S. Sharp, J.M. Becker, R.L. Hettich, Protein surface mapping by chemical oxidation: structural analysis by mass spectrometry, Anal Biochem, 313 (2003) 216-225.
[101] J.S. Sharp, J.M. Becker, R.L. Hettich, Analysis of protein solvent accessible surfaces by photochemical oxidation and mass spectrometry, Anal Chem, 76 (2004) 672-683.

[102] C. Caroline Watson, I. Ireneusz Janik, T. Tiandi Zhuang, O. Olga Charvátová, R.J. Robert J. Woods, J.S. Joshua S. Sharp, Pulsed electron beam water radiolysis for submicrosecond hydroxyl radical protein footprinting, Anal Chem, 81 (2009) 2496-2505.
[103] G.C. Papageorgiou, Photosynthetic activity of diimidoester-modified cells, permeaplasts, and cell-free membrane fragments of the blue-green alga *Anacystis nidulans*, Biochim Biophys Acta, 461 (1977) 379-391.
[104] I. Enami, K. Satoh, S. Katoh, Crosslinking between the 33 kDa extrinsic protein and the 47 kDa chlorophyll-carrying protein of the PS II reaction center core complex, FEBS Lett, 226 (1987) 161-165.
[105] P.A. Millner, G. Gogel, J. Barber, Investigation of the spatial relationships between Photosystem 2 polypeptides by reversible crosslinking and diagonal electrophoresis, Photosyn Res, 13 (1987) 185-198.
[106] I. Enami, Y. Mochizuki, S. Takahashi, T. Kakuno, T. Horio, K. Satoh, S. Katoh, Evidence from crosslinking for the nearest neighbor relationships among the three extrinsic proteins of spinach Photosystem II complexes that are associated with oxygen evolution, Plant Cell Physiol, 31 (1990) 725-729.
[107] I. Enami, S. Ohta, S. Mitsuhashi, S. Takahashi, M. Ikeuchi, S. Katoh, Evidence from crosslinking for a close association of the extrinsic 33 kDa protein with the 9.4 kDa subunit of cytochrome b_{559} and the 4.8 kDa product of the *psb*I gene in oxygen-evolving Photosystem II complexes from spinach, Plant Cell Physiol, 33 (1992) 291-297.
[108] K.-C. Han, J.-R. Shen, M. Ikeuchi, Y. Inoue, Chemical crosslinking studies of extrinsic proteins in cyanobacterial Photosystem II, FEBS Letters, 355 (1994) 121-124.
[109] T. Tomo, K. Satoh, Nearest neighbor analysis of D1 and D2 subunits in the Photosystem II reaction center using a bifunctional cross linker, hexamethylene diisocyanate, FEBS Lett, 351 (1994) 27-30.
[110] R.F. Collins, T.D. Flint, A. Holzenburg, R.C. Ford, T. Thomas, Structural changes in Photosystem II after treatment with the zero-length bifunctional cross-linker 1-ethyl-3-(3-dimethylaminopropyl)carbodiimide: an electron microscopic study, Biochem J, 319 (1996) 585-589.
[111] I. Enami, M. Kamo, H. Ohta, S. Takahashi, T. Miura, M. Kusayanagi, S. Tanabe, A. Kamei, A. Motoki, M. Hirano, T. Tomo, K. Satoh, Intramolecular cross-linking of the extrinsic 33-kDa protein leads to loss of oxygen evolution but not its ability of binding to Photosystem II and stabilization of the manganese cluster, J Biol Chem, 273 (1998) 4629-4634.
[112] I. Enami, S. Yoshihara, A. Tohri, A. Okumura, H. Ohta, J.R. Shen, Cross-reconstitution of various extrinsic proteins and Photosystem II complexes from cyanobacteria, red algae and higher plants, Plant Cell Physiol, 41 (2000) 1354-1364.
[113] R. Nagao, T. Suzuki, A. Okumura, A. Niikura, M. Iwai, N. Dohmae, T. Tomo, J.-R. Shen, M. Ikeuchi, I. Enami, Topological analysis of the extrinsic PsbO, PsbP and PsbQ proteins in a green algal PSII complex by cross-linking with a water-soluble carbodiimide, Plant Cell Physiol, 51 (2010) 718-727.
[114] H. Liu, R.Y.-C. Huang, J. Chen, M.L. Gross, H.B. Pakrasi, Psb27, a transiently associated protein, binds to the chlorophyll binding protein CP43 in Photosystem II assembly intermediates, Proc Natl Acad Sci (USA), 108 (2011) 18536-18541.
[115] H. Liu, H. Zhang, D.M. Niedzwiedzki, M. Prado, G. He, M.L. Gross, R.E. Blankenship, Phycobilisomes supply excitations to both photosystems in a megacomplex in cyanobacteria, Science, 342 (2013) 1104-1107.

[116] K. Ido, J. Nield, Y. Fukao, T. Nishimura, F. Sato, K. Ifuku, Cross-linking evidence for multiple interactions of the PsbP and PsbQ proteins in a higher plant Photosystem II supercomplex, J Biol Chem, 289 (2014) 20150-20157.
[117] H. Liu, H. Zhang, D.A. Weisz, I. Vidavsky, M.L. Gross, H.B. Pakrasi, MS-based cross-linking analysis reveals the location of the PsbQ protein in cyanobacterial Photosystem II, Proc Natl Acad Sci (USA), 111 (2014) 4638-4643.
[118] H. Zhang, H. Liu, D.M. Niedzwiedzki, M. Prado, J. Jiang, M.L. Gross, R.E. Blankenship, Molecular mechanism of photoactivation and structural location of the cyanobacterial Orange Carotenoid Protein, Biochemistry, 53 (2014) 13-19.
[119] O. Tal, B. Trabelcy, Y. Gerchman, N. Adir, Investigation of phycobilisome subunit interaction interfaces by coupled cross-linking and mass spectrometry, J Biol Chem, 289 (2014) 33084-33097.
[120] A. Sinz, Chemical crosslinking and mass spectrometry to map three-dimensional protein structures and protein-protein interactions, Mass Spec Rev, 25 (2006) 663-682.
[121] P. Singh, A. Panchaud, D.R. Goodlett, Chemical cross-linking and mass spectrometry as a low-resolution protein structure determination technique, Anal Chem, (2010) 82.
[122] S.S. Wong, D.M. Jameson, Chemistry of Protein and Nucleic Acid Cross-Linking and Conjugation, Second Edition, CRC Press, 2011.
[123] D. Paramelle, G. Miralles, G. Subra, J. Martinez, Chemical cross-linkers for protein structure studies by mass spectrometry, Proteomics, 13 (2013) 438-456.
[124] B.L. Zybailov, G.V. Glazko, M. Jaiswal, K.D. Raney, Large scale chemical cross-linking mass spectrometry perspectives, J Proteomics Bioinform, S2 (2013) 001.
[125] S. Kalkhof, A. Sinz, Chances and pitfalls of chemical cross-linking with amine-reactive N-hydroxysuccinimide esters, Anal Bioanal Chem, 392 (2008) 305-312.
[126] S. Mädler, C. Bich, T. Touboul, R. Zenobi, Chemical cross-linking with NHS esters: a systematic study on amino acid reactivities, J Mass Spec, 44 (2009) 694-706.
[127] I. Migneault, C. Dartiguenave, M.J. Bertrand, K.C. Waldron, Glutaraldehyde: behavior in aqueous solution, reaction with proteins, and application to enzyme crosslinking, Biotechniques, 37 (2004) 790-802.
[128] B.W. Sutherland, J. Toews, J. Kast1, Utility of formaldehyde cross-linking and mass spectrometry in the study of protein–protein interactions, J Mass Spec, 43 (2008) 699-715.
[129] M.-H. Kuo, C.D. Allis, In vivo cross-Linking and immunoprecipitation for studying dynamic protein:DNA associations in a chromatin environment, Methods, 19 (1999) 425-433.
[130] T.S. Furey, ChIP–seq and beyond: new and improved methodologies to detect and characterize protein–DNA interactions, Nat Rev Genet, 13 (2012) 840-852.
[131] J. Toewsa, J.C. Rogalskib, T.J. Clark, J. Kasta, Mass spectrometric identification of formaldehyde-induced peptide modifications under *in vivo* protein cross-linking conditions, Anayl Chim Acta, (2008) 168-183.
[132] C. Klockenbusch, J.E. O'Hara, J. Kast, Advancing formaldehyde cross-linking toward quantitative proteomic applications, Anal Bioanal Chem, 404 (2012) 1057-1067.
[133] A.N. Glazer, Phycobilisome: assembly and structure, Elsevier, Amsterdam, The Netherlands, 1987.
[134] M. Mimuro, H. Kikuchi, Cyanophyta and Rhodophyta, Kluwer Academic Publishers, Dordrecht, The Netherlands, 2003.
[135] C.W. Mullineaux, Phycobilisome-reaction centre interaction in cyanobacteria, Photosyn Res, 95 (2008) 175-182.

[136] A.A. Arteni, G. Ajlani, E.J. Boekema, Structural organisation of phycobilisomes from *Synechocystis* sp. strain PCC6803 and their interaction with the membrane, Biochim Biophys Acta, 1787 (2009) 272-279.
[137] N. Adir, Elucidation of the molecular structures of components of the phycobilisome: reconstructing a giant, Photosyn Res, 85 (2005) 15-32.
[138] M. Watanabe, M. Ikeuchi, Phycobilisome: architecture of a light-harvesting supercomplex, Photosyn Res, 116 (2013) 265-276.
[139] A.C. Ley, W.L. Butler, The distrubution of excitetion energy between Photosystem I and Photosystem II in *Porphyridium cruentum*, Japan Soc. of Plant Physiology, Tokyo, 1977.
[140] A.C. Ley, W.L. Butler, Energy distribution in the photochemical apparatus of *Porphyridium cruentum* in State I and State II Biochim Biophys Acta, 592 (1980) 349-363.
[141] J. Biggins, D. Bruce, Regulation of excitation energy transfer in organisms containing phycobilins, Photosyn Res, 20 (1989) 1-34.
[142] H.J.M. Kramer, W.H.J. Westerhuis, J. Amesz, Low temperature spectroscopy of intact algae, Physiol Veg, 23 (1985) 535-543.
[143] C.W. Mullineaux, Excitation energy transfer from phycobilisomes to Photosystem I in a cyanobacterium., Biochim Biophys Acta, 1100 (1992) 285-292.
[144] J. Zhao, J. Zhou, D.A. Bryant, Energy transfer processes in phycobilisomes as deduced from analyses of mutants of *Synechococcus* sp. PCC 7002, Kluwer Academic Publishers, Dordrecht, The Netherlands, 1992.
[145] A.N. Glazer, Y.M. Gindt, C.F. Chan, K. Sauer, Selective disruption of energy flow from phycobilisomes to Photosystem I, Photosyn Res, 40 (1994) 167-173.
[146] T.M. Bricker, J. Morvant, N. Masri, H. Sutton, L.K. Frankel, Isolation of a highly active Photosystem II preparation from *Synechocystis* 6803 using a histidine-tagged mutant of CP 47, Biochim Biophys Acta, 1409 (1998) 50-57.
[147] K. El Bissati, E. Delphin, N. Murata, A. Etienne, D. Kirilovsky, Photosystem II fluorescence quenching in the cyanobacterium *Synechocystis* PCC 6803: involvement of two different mechanisms, Biochim Biophys Acta, 1457 (2000) 229-242.
[148] M.G. Rakhimberdieva, I.N. Stadnichuk, I.V. Elanskaya, N.V. Karapetyan, Carotenoid induced quenching of the phycobilisome fluorescence in Photosystem II-deficient mutant of *Synechocystis* sp., FEBS Lett, 574 (2004) 85-88.
[149] A. Wilson, G. Ajlani, J.M. Verbavatz, I. Vass, C.A. Kerfeld, D. Kirilovsky, A soluble carotenoid protein involved in phycobilisome-related energy dissipation in cyanobacteria, Plant Cell, 18 (2006) 992-1007.
[150] T.K. Holt, D.W. Krogmann, A carotenoid-protein from cyanobacteria, Biochim Biophys Acta, 637 (1981) 408-414.
[151] T. Polivka, C.A. Kerfeld, T. Pascher, V. Sundström, Spectroscopic properties of the carotenoid 3′-hydroxyechinenone in the orange carotenoid protein from the cyanobacterium *Arthrospira maxima*, Biochemistry, 44 (2005) 3994-4003.
[152] D. Kirilovsky, C.A. Kerfeld, The orange carotenoid protein in photoprotection of Photosystem II in cyanobacteria, Biochim Biophys Acta, 1817 (2013) 158-166.
[153] A. Wilson, J. Kinney, P.H. Zwart, C. Punginelli, S. D'Haen, F. Perreau, M.G. Klein, D. Kirilovsky, C.A. Kerfeld, Structural determinants underlying photoprotection in the photoactive orange carotenoid protein of cyanobacteria, J Biol Chem, 285 (2010) 18364-18375.

[154] M. Sutter, C.A. Kerfeld, Crystal structure of the FRP and identification of the active site for modulation of OCP-mediated photoprotection in cyanobacteria, Proc Natl Acad Sci (USA), 110 (2013) 10022-10027.
[155] A.J.R. Heck, R.H.H. van den Heuvel, Investigation of intact protein complexes by mass spectrometry, Mass Spec Rev, 23 (2004) 368-389.
[156] M. Gwizdala, A. Wilson, D. Kirilovsky, *In vitro* reconstitution of the cyanobacterial photoprotective mechanism mediated by the Orange Carotenoid Protein in *Synechocystis* PCC 6803, Plant Cell, 23 (2011) 2631-2643.
[157] R.L. Leverenz, M. Sutter, A. Wilson, S. Gupta, A. Thurotte, C. Bourcier de Carbon, C.J. Petzold, C. Ralston, F. Perreau, D. Kirilovsky, K. C.A., A 12 Å carotenoid translocation in a photoswitch associated with cyanobacterial photoprotection, Science, 348 (2015) 1463-1466.
[158] T.M. Bricker, J.L. Roose, P. Zhang, L.K. Frankel, The PsbP family of proteins, Photosyn Res, 116 (2013) 235-250.
[159] L. Thornton, H. Ohkawa, J. Roose, Y. Kashino, N. Keren, H. Pakrasi, Homologs of plant PsbP and PsbQ proteins are necessary for regulation of Photosystem II activity in the cyanobacterium *Synechocystis* 6803, Plant Cell, 16 (2004) 2164-2175.
[160] Y. Ishikawa, W.P. Schroder, C. Funk, Functional analysis of the PsbP-like protein (*sll*1418) in *Synechocystis* sp. PCC 6803, Photosyn Res, 84 (2005) 257-262.
[161] F. Michoux, M. Boehm, W. Bialek, K. Takasaka, K. Maghlaoui, J. Barber, J.W. Murray, P.J. Nixon, Crystal structure of CyanoQ from the thermophilic cyanobacterium *Thermosynechococcus elongatus* and detection in isolated Photosystem II complexes, Photosyn Res, 122 (2014) 57-67.
[162] J.L. Roose, Y. Kashino, H.B. Pakrasi, The PsbQ protein defines cyanobacterial Photosystem II complexes with highest activity and stability, Proc Natl Acad Sci (USA), 104 (2007) 2548-2553.
[163] H. Liu, D.A. Weisz, H.B. Pakrasi, Multiple copies of the PsbQ protein in a cyanobacterial Photosystem II assembly intermediate complex, Photosyn Res, (2015).
[164] N. Bondarava, P. Beyer, A. Krieger-Liszkay, Function of the 23 kDa extrinsic protein of Photosystem II as a manganese binding protein and its role in photoactivation., Biochim Biophys Acta, 1708 (2005) 63-70.
[165] N. Bondarava, A. Krieger-Liszkay, Manganese binding to the 23 kDa extrinsic protein of Photosystem II., Biochim Biophys Acta, 1767 (2007) 583-588.
[166] J. Nield, M. Balsera, J. De Las Rivas, J. Barber, Three-dimensional electron cryo-microscopy study of the extrinsic domains of the oxygen-evolving complex of spinach: assignment of the PsbO protein, J Biol Chem, 277 (2002) 15006-15012.
[167] K. Ido, S. Kakiuchi, C. Uno, T. Nishimura, Y. Fukao, T. Noguchi, F. Sato, K. Ifuku, The conserved His-144 in the PsbP protein is important for the interaction between the PsbP N-terminus and the Cyt b_{559} subunit of Photosystem II, J Biol Chem, 287 (2012) 26377–26387.
[168] K. Ifuku, F. Sato, Importance of the N-terminal sequence of the extrinsic 23 kDa polypeptide in Photosystem II in ion retention in oxygen evolution, Biochim Biophys Acta, 1546 (2001) 196-204.
[169] K. Ifuku, F. Sato, A truncated mutant of the extrinsic 23-kDa protein that absolutely requires the extrinsic 17-kDa protein for Ca^{2+} retention in Photosystem II, Plant Cell Physiol, 43 (2002) 1244-1249.
[170] J. Kopecky, V., J. Kohoutova, M. Lapkouski, K. Hofbauerova, Z. Sovova, O. Ettrichova, S. González-Pérez, A. Dulebo, D. Kaftan, I.K. Smatanova, J.L. Revuelta, J.B. Arellano, J. Carey,

R. Ettrich Raman spectroscopy adds complementary detail to the high-resolution X-ray crystal structure of photosynthetic PsbP from *Spinacia oleracea*, Plos One, 7 (2012) e46694.
[171] G.T. Hermanson, Bioconjugate Techniques, Academic Press, San Diego, CA, 1996.
[172] S. Kalkhoh, A. Sinz, Chances and pitfalls of chemical crosslinking with amine-reactive *N*-hydroxysuccinimide esters, Anal Bioanal Chem, 392 (2008) 305-312.
[173] K. Ifuku, Localization and functional characterization of the extrinsic subunits of Photosystem II: an update, Biosci Biotechnol Biochem, (2015).
[174] F.M. Ho, Structural and mechanistic investigations of Photosystem II through computational methods, Biochim Biophys Acta, 1817 (2012) 106-120.
[175] M. Petřek, M. Otyepka, P. Banáš, P. Košinová, J. Koča, CAVER: A new tool to explore routes from protein clefts, pockets and cavities, BMC Bioinform, 7 (2006) 315-315.
[176] F.M. Ho, S. Styring, Access channels and methanol binding site to the $CaMn_4$ cluster in Photosystem II based on solvent accessibility simulations, with implications for substrate water access, Biochim Biophys Acta, 1777 (2008) 140-153.
[177] S. Vassiliev, P. Comte, A. Mahoob, D. Bruce, Tracking the flow of water through PS II using molecular dynamics and streamline tracing, Biochemistry, 49 (2010) 1873-1881.
[178] S. Vassiliev, T. Zaraiskaya, D. Bruce, Exploring the energetics of water permeation in Photosystem II by multiple steered molecular dynamics simulations, Biochim Biophys Acta, 1817 (2012) 1671-1678.
[179] J.W. Murray, J. Barber, Structural characteristics of channels and pathways in Photosystem II including the identification of an oxygen channel, J Struct Biol, 159 (2007) 228-237.
[180] A. Gabdulkhakov, A. Guskov, A.M. Broser, J. Kern, F. Müh, W. Saenger, A. Zouni, Probing the accessibility of the Mn_4Ca cluster in Photosystem II; channels calculation, noble gas derivatization, and cocrystallization with DMSO, Structure, 17 (2009) 1223-1234.
[181] H. Michel, D.F. Hunt, J. Shabanowitz, J. Bennett, Tandem mass spectrometry reveals that three Photosystem II proteins of spinach chloroplasts contain *N*-acetyl-*0*-phosphothreonine at their NH_2 termini, J Biol Chem, 263 (1988) 1123-1130.
[182] H. Michel, J. Bennett, Identification of the phosphorylation site of an 8.3 kDa protein from Photosystem II of spinach, FEBS Lett, 212 (1987) 103-108.
[183] A.V. Vener, A. Harms, M.R. Sussman, R.D. Vierstra, Mass spectrometric resolution of reversible protein phosphorylation in photosynthetic membranes of *Arabidopsis thaliana*, J Biol Chem, 276 (2001) 6959-6966.
[184] M. Hansson, A.V. Vener, Identification of three previously unknown *in vivo* protein phosphorylation sites in thylakoid membranes of *Arabidopsis thaliana*, Mol Cell Proteom, 2 (2003) 550-559.
[185] M.V. Turkina, J. Kargul, A. Blanco-Rivero, A. Villarejo, J.B. Barber, A.V. Vener, Environmentally modulated phosphoproteome of photosynthetic membranes in the green alga *Chlamydomonas reinhardtii*, Mol Cell Proteom, 5 (2006) 1412-1425.
[186] A.V. Vener, Phosphorylation of thylakoid proteins, in: B. Demmig-Adams, W. Adams, A.K. Mattoo (Eds.) Photoprotection, Photoinhibition, Gene Regulation and Environment, Springer, Dordrecht, The Netherlands, 2006, pp. 107-126.
[187] M. Tikkenen, E.-M. Aro, Thylakoid protein phosphorylation in dynamic regulation of Photosystem II in higher plants, Biochim Biophys Acta, 1817 (2012) 232-238.
[188] S. Puthiyaveetil, H. Kirchhoff, A phosphorylation map of the Photosystem II supercomplex C2S2M2, Front Plant Sci, 4 (2013) 459.

[189] S. Reiland, G. Messerli, K. Baerenfaller, B. Gerrits, A. Endler, J. Grossmann, W. Gruissem, S. Baginsky, Large-scale arabidopsis phosphoproteome profiling reveals novel chloroplast kinase substrates and phosphorylation networks, Plant Physiol, 150 (2009) 889-903.
[190] K. Lohrig, B. Müller, J. Davydova, D. Leister, D.A. Wolters, Phosphorylation site mapping of soluble proteins: bioinformatical filtering reveals potential plastidic phosphoproteins in *Arabidopsis thaliana*, Planta, 229 (2009) 1123-1134.
[191] V. Wagner, G. Geßner, I. Heiland, M. Kaminski, S. Hawat, K. Scheffler, M. Mittag, Analysis of the phosphoproteome of *Chlamydomonas reinhardtii* provides new insights into various cellular pathways, Eukary Cell, 5 (2006) 457-468.
[192] J. Nickelsen, B. Rengstl, Photosystem II assembly: from cyanobacteria to plants, Ann Rev Plant Biol, 64 (2013) 609-635.
[193] A. Melis, Photosystem II damage and repair cycle in chloroplasts: what modulates the rate of photodamage *in vivo*?, Trends Plant Science, 4 (1999) 1360-1385.
[194] I. Vass, Molecular mechanisms of photodamage in the Photosystem II complex, Biochim Biophys Acta, 1817 (2012) 209-217.
[195] K. Nath, A. Jajoo, R.S. Sharma Poudyal, R. Timilsina, Y.S. Park, E.-M. Aro, H.G. Nam, C.-H. Lee, Towards a critical understanding of the Photosystem II repair mechanism and its regulation during stress conditions, FEBS Lett, 587 (2013) 3372-3381.
[196] N. Murata, S. Takahashi, Y. Nishiyama, S.I. Allakhverdiev, Photoinhibition of Photosystem II under environmental stress, Biochim Biophys Acta, 1767 (2007) 414-421.
[197] Y. Nishiyama, N. Murata, Revised scheme for the mechanism of photoinhibition and its application to enhance the abiotic stress tolerance of the photosynthetic machinery, App Microbiol Biotechnol, 98 (2014) 8777-8796.
[198] J.R. Durrant, L.B. Giorgi, J. Barber, D.R. Klug, G. Porter, Characterization of triplet-states in isolated Photosystem II reaction centres - oxygen quenching as a mechanism for photodamage, Biochim Biophys Acta, 1017 (1990) 166-175.
[199] A.N. Macpherson, A. Telfer, T.G. Truscott, J. Barber Direct detection of singlet oxygen from isolated Photosystem II reaction centres, Biochim Biophys Acta, 1143 (1993) 301-309.
[200] E. Hideg, C. Spetea, I. Vass, Singlet oxygen production in thylakoid membranes during photoinhibition as detected by EPR spectroscopy, Photosyn Res, 39 (1994) 191-199.
[201] D.J. Kyle, I. Ohad, C.J. Arntzen, Membrane protein damage and repair: selective loss of a quinone-protein function in chloroplast membranes, Proc Natl Acad Sci (USA), 81 (1984) 4070-4074.
[202] G.M. Ananyev, G. Renger, U. Wacker, V. Klimov, The photoproduction of superoxide radicals and the superoxide dismutase activity of Photosystem II. The possible involvement of cytochrome b_{559}, Photosyn Res, (1994) 327-338.
[203] K. Liu, J. Sun, Y.G. Song, B. Liu, Y.K. Xu, S.X. Zhang, Q. Tian, Y. Liu, Superoxide, hydrogen peroxide and hydroxyl radical in D1/D2/cytochrome b_{559} Photosystem II reaction center complex, Photosyn Res, 81 (2004) 41-47.
[204] J. Whitmarsh, H.B. Pakrasi, Form and function of cytochrome b_{559}, in: D.R. Ort, C.F. Yocum (Eds.) Oxygenic Photosynthesis: The Light Reactions, Kluwer Academic Publishers, Dordrech, 1996, pp. 249-264.
[205] J. Kruk, K. Strzałka, Dark reoxidation of the plastoquinone-pool is mediated by the low-potential form of cytochrome b_{559} in spinach thylakoids, Photosyn Res, 62 (1999) 273-279.

[206] J. Sharma, M. Panico, J. Barber, H.R. Morris, Purification and determination of intact molecular mass by electrospray ionization mass spectrometry of the Photosystem II reaction center subunits, J Biol Chem, 272 (1997) 33153-33157.
[207] T.M. Dreaden, J. Chen, S. Rexroth, B.A. Barry, N-Formylkynurenine as a marker of high light stress in photosynthesis, J Biol Chem, 286 (2011) 22632-22641.
[208] T.M. Dreaden-Kasson, S. Rexroth, B.A. Barry, Light-induced oxidative stress, *N*-formylkynurenine, and oxygenic photosynthesis, Plos One, 7 (2012) e42220.
[209] A. Gieβauf, B. van Wickern, T. Simat, H. Steinhart, H. Esterbauer, Formation of N-formylkynurenine suggests the involvement of apolipoprotein B-100 centered tryptophan radicals in the initiation of LDL lipid peroxidation, FEBS Lett, 389 (1996) 136-140.
[210] M. Gracanin, C.L. Hawkins, D. Pattison, M.J. Davies, Singlet-oxygen-mediated amino acid and protein oxidation: formation of tryptophan peroxides and decomposition products, Free Radic Biol Med, 47 (2009) 92-102.
[211] P. Guptasarma, D. Balasubramanian, S. Matsugo, I. Saito, Hydroxyl radical mediated damage to proteins, with special reference to the crystallins, Biochemistry, 31 (1992) 4296–4303.
[212] L.B. Anderson, M. Maderia, A.J.A. Ouellette, C. Putnam-Evans, L. Higgins, T. Krick, M.J. MacCoss, H. Lim, J.R. Yates III, B.A. Barry, Posttranslational modifications in the CP43 subunitof Photosystem II, Proc Natl Acad Sci (USA), 99 (2002) 14676-14681.
[213] M. Sugiura, K. Koyama, Y. Umena, K. Kawakami, J.-R. Shen, N. Kamiya, A. Boussac, Evidence for an unprecedented histidine hydroxyl modification on D2-His336 in Photosystem II of *Thermosynechoccocus vulcanus* and *Thermosynechoccocus elongatus*, Biochemistry, 52 (2013) 9246-9431.
[214] P.D. Mabbitt, G.J.P. Rautureau, C.L. Day, S.M. Wilbanks, J.J. Eaton-Rye, M.G. Hinds, Solution structure of Psb27 from cyanobacterial Photosystem II, Biochemistrty, 48 (2009) 8771-8773.
[215] W.J. Bialek, S. Wen, F. Michoux, M. Beckova, J. Komenda, J.W. Murray, P.J. Nixon, Crystal structure of the Psb28 assembly factor of *Thermosynechococcus elongatus* Photosystem II at 2.3 Å, Photosyn Res, 117 (2013) 375-383.
[216] J.L. Roose, H.B. Pakrasi, The Psb27 protein facilitates manganese cluster assembly in Photosystem II, J Biol Chem, 283 (2007) 4044-4050.
[217] M.M. Nowaczyk, R. Hebeler, E. Schlodder, H.E. Meyer, B. Warscheid, M. Rogner, Psb27, a cyanobacterial lipoprotein, is involved in the repair cycle of Photosystem II, Plant Cell, 18 (2006) 3121-3131.
[218] H. Liu, J.L. Roose, J.C. Cameron, H.B. Pakrasi, A genetically tagged Psb27 protein allows purification of two consecutive Photosystem II (PSII) assembly intermediates in *Synechocystis* 6803, a cyanobacterium, J Biol Chem, 286 (2011) 24865–24871.
[219] J. Bruce, *In vivo* protein complex topologies: Sights through a cross-linking lens, Proteomics, 12 (2012) 1565-1575.
[220] M.J. Solomon, A. Varshavsky, Formaldehyde-mediated DNA-protein crosslinking: a probe for *in vivo* chromatin structures, Proc Natl Acad Sci (USA), 82 (1985) 6470-6474.
[221] V. Orlando, H. Strutt, R. Paro, Analysis of chromatin structure by *in vivo* formaldehyde cross-linking, Methods, 11 (1997) 205-215.
[222] L. Feiz, R. Williams-Carrier, K. Wostrikoff, S. Belcher, A. Barkan, D.B. Stern, Ribulose-1,5-bis phosphate carboxylase/oxygenase accumulation factor 1 is required for holoenzyme assembly in maize, Plant Cell, 24 (2012) 3435-3446.

[223] T.C. Currier, J.F. Haury, C.P. Wolk, Isolation and preliminary characterization of auxotrophs of a filamentous cyanobacterium, J Bacteriol, 129 (1977) 1556-1562.
[224] G. Yamanaka, A.N. Glazer, Dynamic aspects of phycobilisome structure: Phycobilisome turnover during nitrogen starvation in *Synechococcus* sp., Arch Microbiol, 124 (1980) 39-47.
[225] N. Tandeau de Marsac, W.E. Borrias, C.J. Kuhlemeier, A.M. Casetes, G.A. van Arkel, C.A.M.J.J. van den Hondel, A new approach for molecular cloning in cyanobacteria: cloning of an *Anacystis nidulans met* gene using a Tn-901-induced mutant, Gene 20 (1982) 111-119.
[226] L.N. Nefedova, V.A. Mel'nik, M.M. Babykin, Mutants of cyanobacterium *Synechocystis* sp PCC6803 with insertion of the *sod*B gene encoding Fe-superoxide dismutase, Genetika, 39 (2003) 478-482.
[227] A. Schulz, P. Sponemann, H. Kocher, F. Wengenmayer, The herbicidally active experimental compound Hoe 704 is a potent inhibitor of the enzyme acetolactate reductoisomerase, FEBS Lett, 238 (1988) 375-378.
[228] V.A. Wittenbach, D.R. Rayner, J.V. Schloss, Pressure points in the biosynthetic pathway for branched-chain amino acids, in: R.K. Singh, H.E. Flores, J.C. Shannon (Eds.) Biosynthesis and Molecular Regulation of Amino acids in Plants, American Society of Plant Physiologists, Rockville, MD (USA), 1991, pp. 69-88.

Figure 1

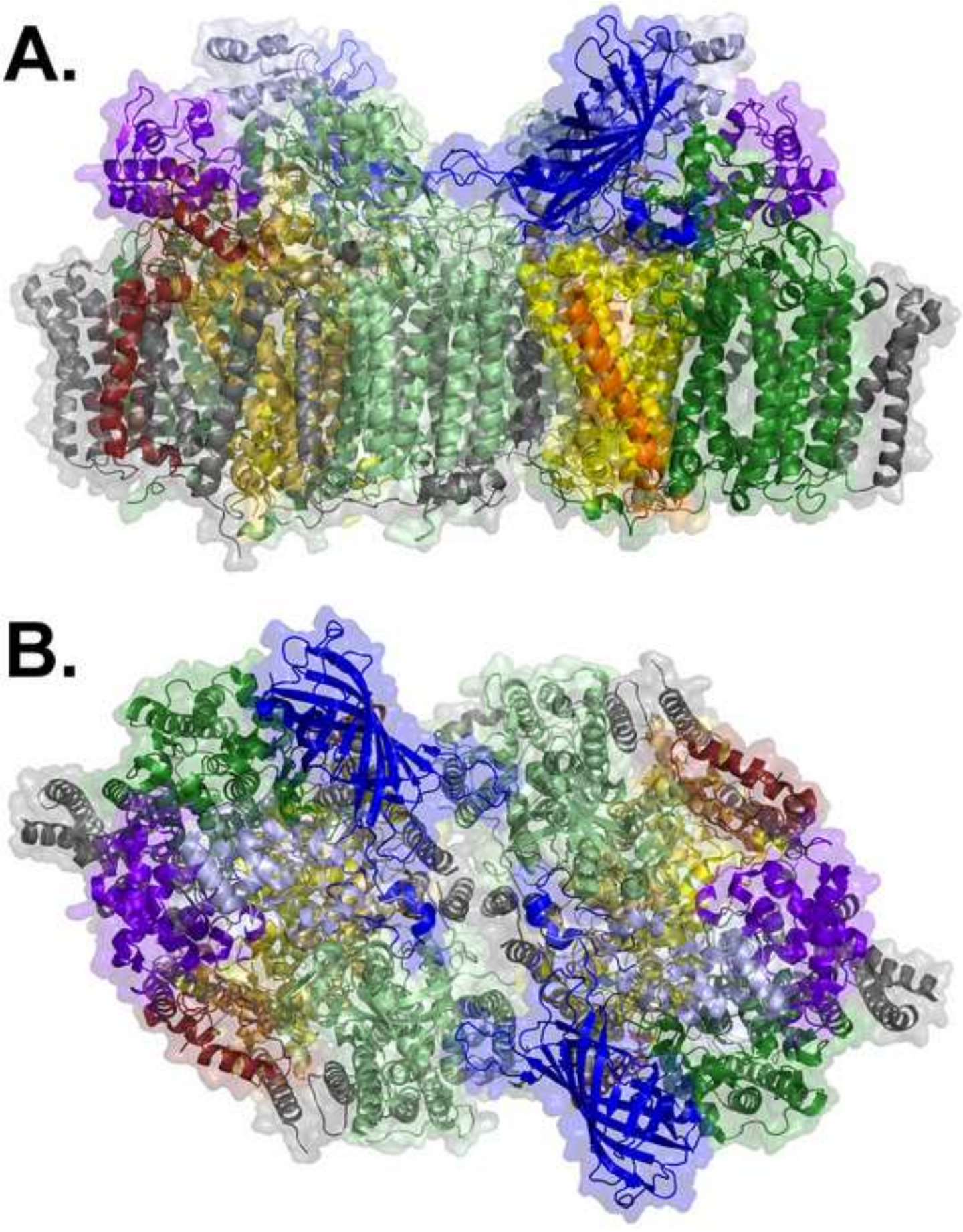

Figure 2

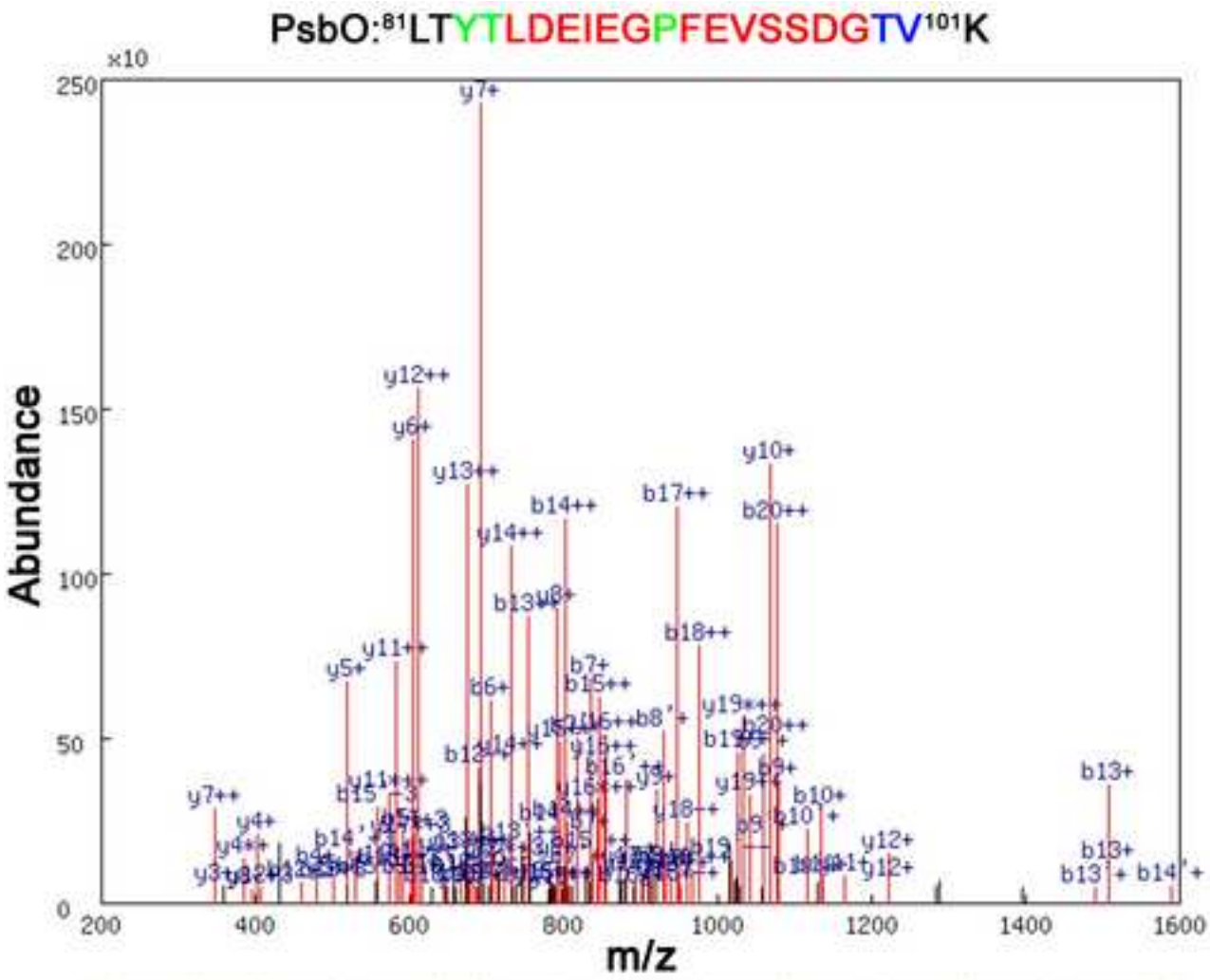

#	b'++	b*++	b++	b'+	b*+	b+	seq	y'++	y*++	y++	y'+	y*+	y+	#
1			57.55			114.09	L	1141.56	1142.05	1150.56	2282.11	2283.09	2300.12	M
2	99.07		108.07	197.13		215.14	T	1085.02	1085.51	1094.02	2169.02	2170.01	2187.03	20
3	180.60		189.60	360.19		378.20	Y	1034.49	1034.98	1043.50	2067.98	2068.96	2085.99	19
4	231.12		240.13	461.24		479.25	T	952.96	953.45	961.97	1904.91	1905.90	1922.92	18
5	287.67		296.67	574.32		592.33	L	902.44	902.93	911.44	1803.86	1804.85	1821.88	17
6	345.18		354.18	689.35		707.36	D	845.89	846.39	854.90	1690.78	1691.76	1708.79	16
7	409.70		418.71	818.39		836.40	E	788.38	788.87	797.39	1575.75	1576.74	1593.76	15
8	466.24		475.25	931.48		949.49	I	723.86	724.35	732.86	1446.71	1447.70	1464.72	14
9	530.76		539.77	1060.52		1078.53	E	667.32	667.81	676.32	1333.63	1334.61	1351.64	13
10	559.27		568.28	1117.54		1135.55	G	602.80	603.29	611.80	1204.58	1205.57	1222.60	12
11	607.80		616.81	1214.59		1232.60	P	574.29	574.78	583.29	1147.56	1148.55	1165.57	11
12	681.33		690.34	1361.66		1379.67	F	525.76	526.25	534.76	1050.51	1051.49	1068.52	10
13	745.86		754.86	1490.70		1508.72	E	452.22	452.72	461.23	903.44	904.43	921.45	9
14	795.39		804.40	1589.77		1607.78	V	387.70	388.20	396.71	774.40	775.38	792.41	8
15	838.91		847.91	1676.81		1694.82	S	338.17	338.66	347.17	675.33	676.31	693.34	7
16	882.42		891.43	1763.84		1781.85	S	294.65	295.15	303.66	588.30	589.28	606.31	6
17	939.94		948.94	1878.86		1896.87	D	251.14	251.63	260.14	501.27	502.25	519.28	5
18	968.45		977.45	1935.89		1953.90	G	193.62	194.12	202.63	386.24	387.22	404.25	4
19	1018.97		1027.98	2036.93		2054.94	T	165.11	165.60	174.12	329.22	330.20	347.23	3
20	1068.50		1077.51	2136.00		2154.01	V	114.59	115.08	123.59	228.17	229.15	246.18	2
							K	65.05	65.55	74.06	129.10	130.09	147.11	1

Figure 3

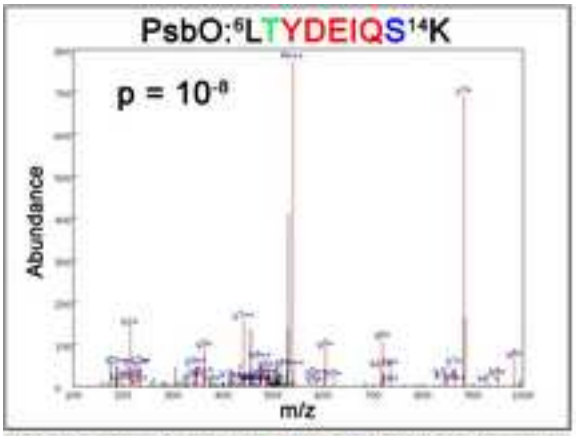
PsbO:⁶LTYDEIQS¹⁴K
p = 10⁻⁸
Abundance
m/z

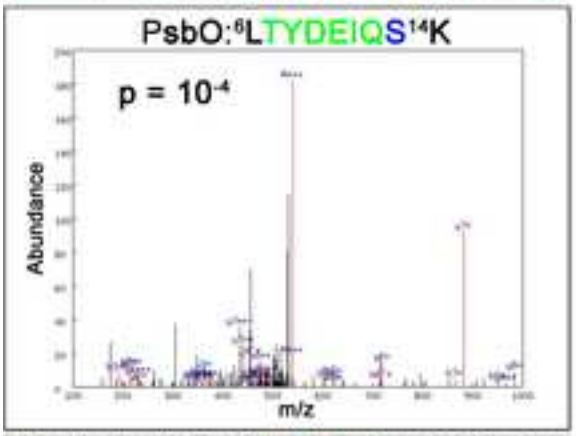
PsbO:⁶LTYDEIQS¹⁴K
p = 10⁻⁴
Abundance
m/z

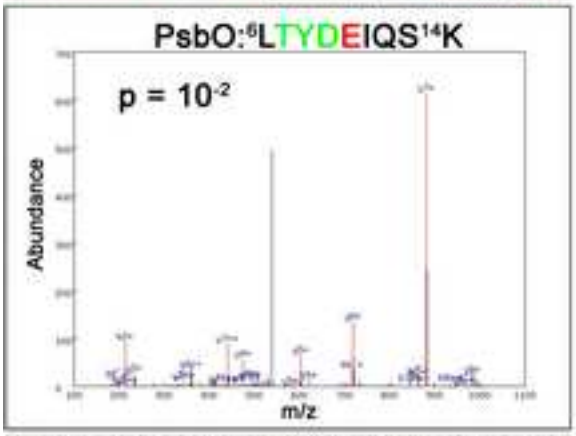
PsbO:⁶LTYDEIQS¹⁴K
p = 10⁻²
Abundance
m/z

Figure 4

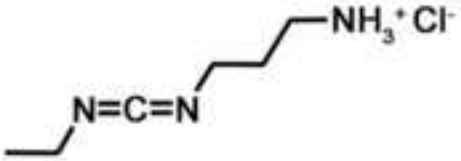

1-ethyl-3-(3-dimethylaminopropyl)carbodiimide • HCl
(EDC, 0.0 Å)

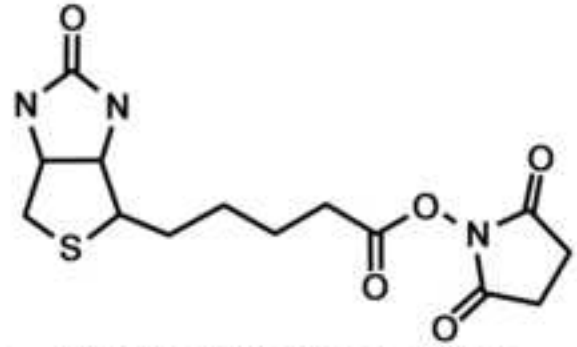

N-hydroxysuccinimidobiotin
(NHS-biotin)

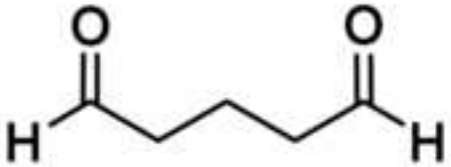

Gluteraldehyde
(GA, 7.7 Å)

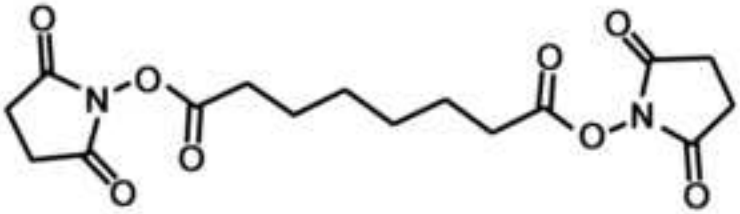

Disuccinimidyl suberate
(DSS, 11.4 Å)

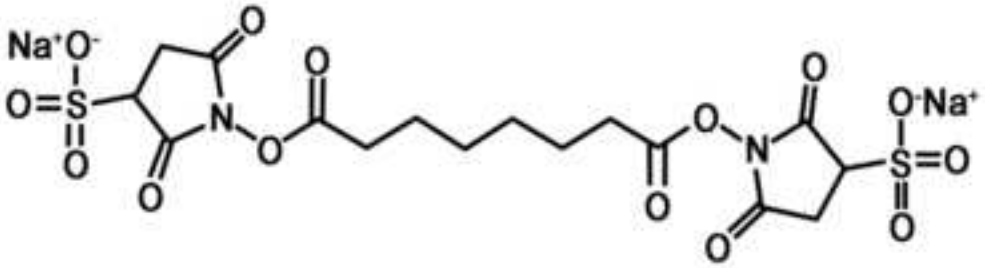

Bis(sulfosuccinimidyl) suberate
(BS3, 11.4 Å)

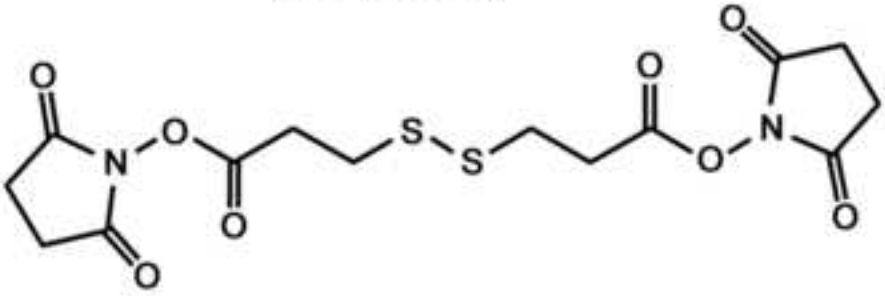

Dithiobis(succinimidyl propionate)
(DSP, 12.0 Å)

Figure 5

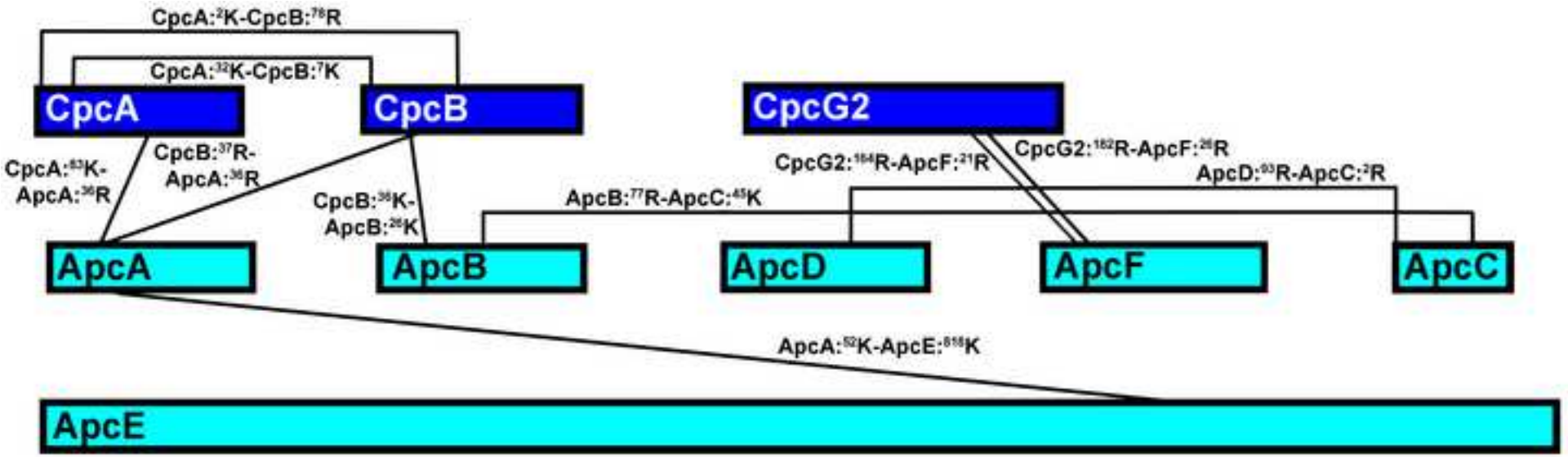
CpcA:2K-CpcB:76R
CpcA:32K-CpcB:7K
CpcA
CpcB
CpcG2
CpcA:83K-
ApcA:36R
CpcB:37R-
ApcA:36R
CpcB:36K-
ApcB:26K
CpcG2:164R-ApcF:21R
CpcG2:162R-ApcF:26R
ApcD:93R-ApcC:2R
ApcB:77R-ApcC:45K
ApcA
ApcB
ApcD
ApcF
ApcC
ApcA:52K-ApcE:818K
ApcE

Figure 6

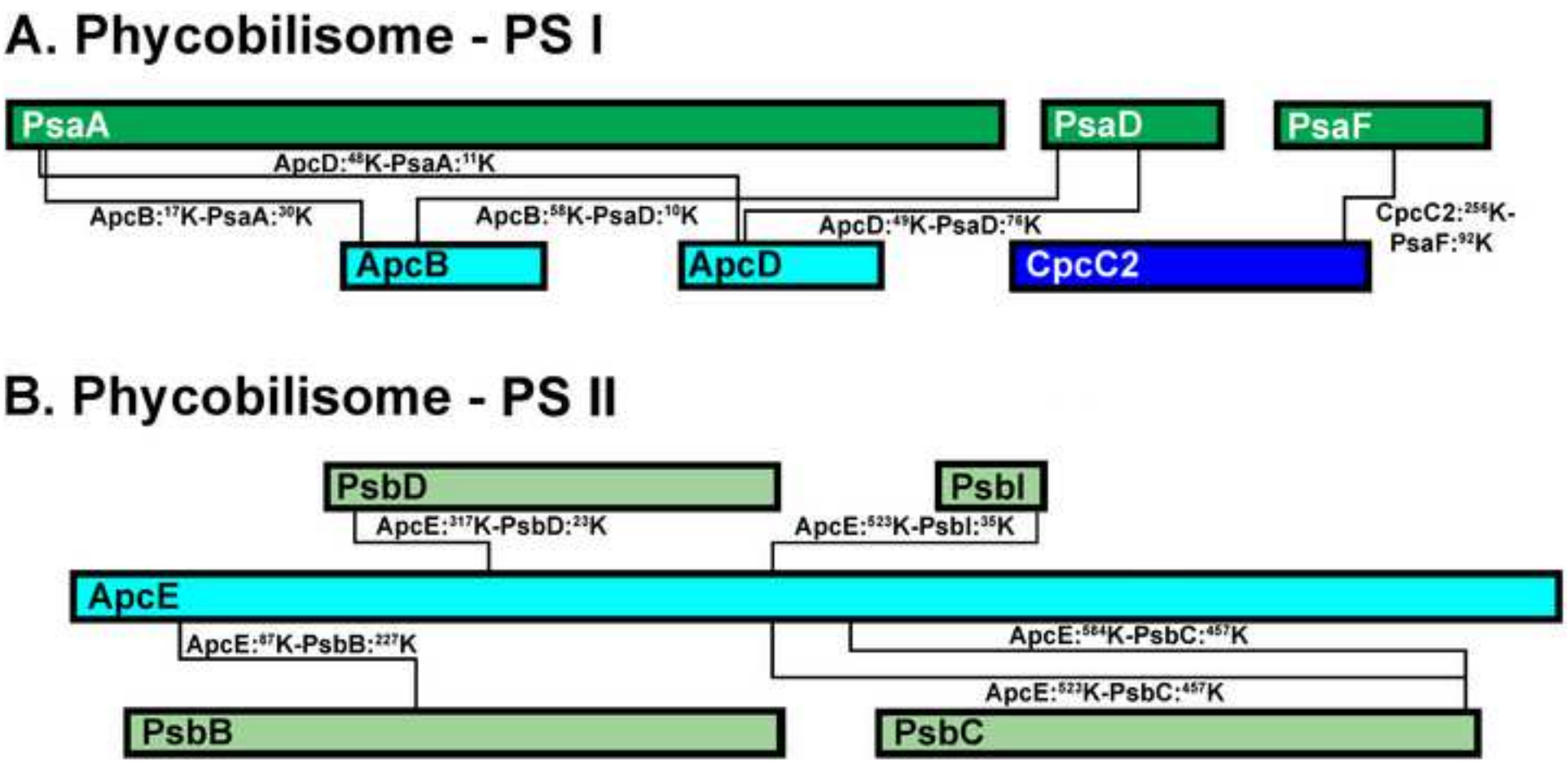
A. Phycobilisome - PS I
PsaA
PsaD
PsaF
ApcD:48K-PsaA:11K
ApcB:17K-PsaA:30K
ApcB:58K-PsaD:10K
ApcD:49K-PsaD:76K
CpcC2:256K-PsaF:92K
ApcB
ApcD
CpcC2
B. Phycobilisome - PS II
PsbD
PsbI
ApcE:317K-PsbD:23K
ApcE:523K-PsbI:35K
ApcE
ApcE:87K-PsbB:227K
ApcE:564K-PsbC:457K
ApcE:523K-PsbC:457K
PsbB
PsbC

Figure 7

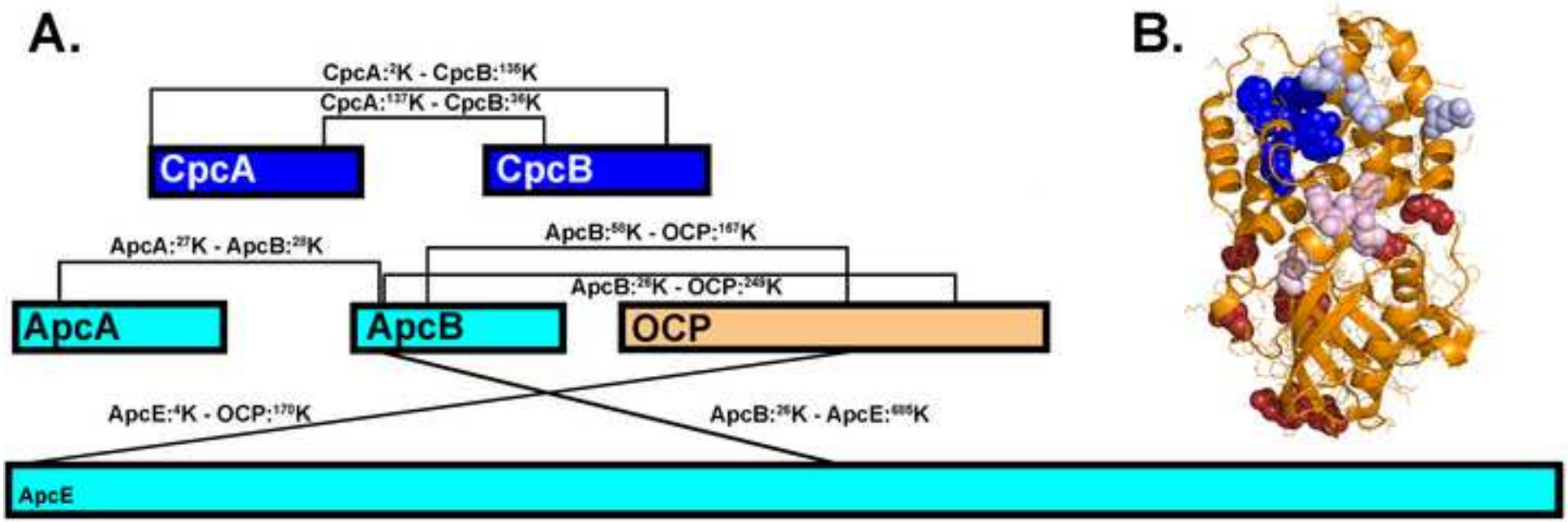
A.
CpcA:2K - CpcB:135K
CpcA:137K - CpcB:36K
CpcA
CpcB
ApcA:27K - ApcB:28K
ApcB:58K - OCP:167K
ApcB:28K - OCP:249K
ApcA
ApcB
OCP
ApcE:4K - OCP:170K
ApcB:26K - ApcE:685K
ApcE
B.

Figure 8

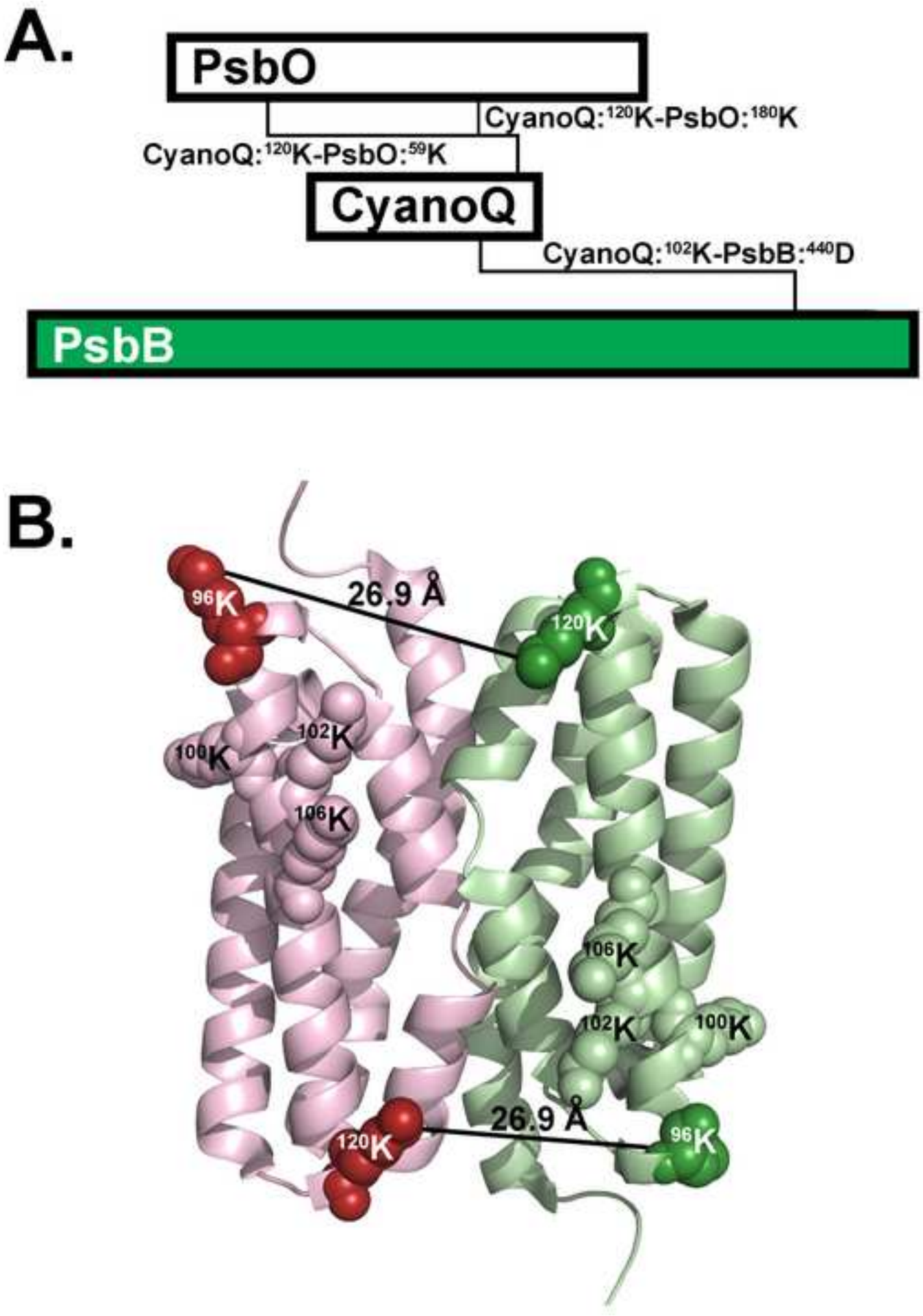
A.
PsbO
CyanoQ:120K-PsbO:180K
CyanoQ:120K-PsbO:59K
CyanoQ
CyanoQ:102K-PsbB:440D
PsbB
B.
96K
26.9 Å
120K
102K
100K
106K
106K
102K
100K
26.9 Å
120K
96K

Figure 9

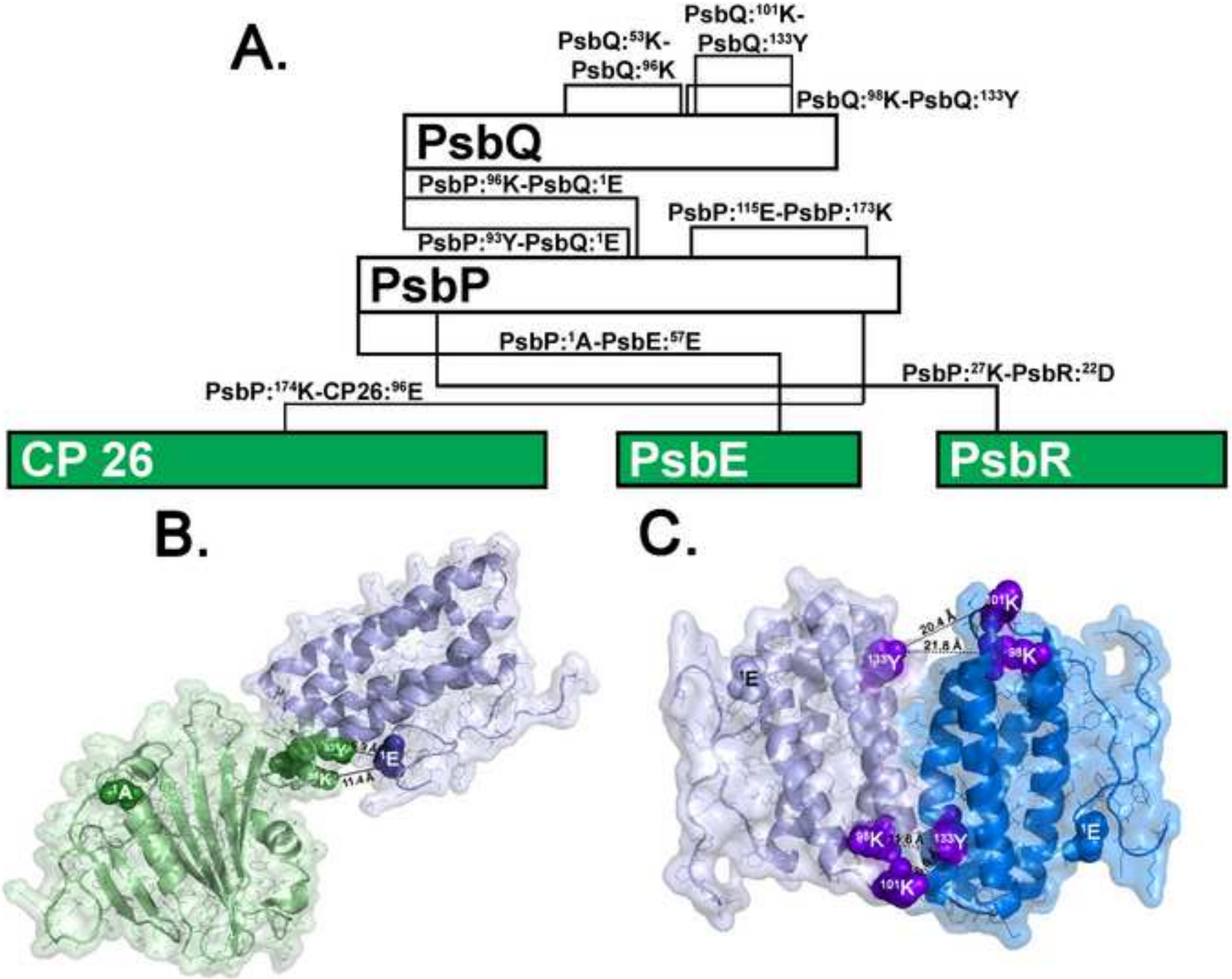
A.
PsbQ:101K-
PsbQ:53K-
PsbQ:133Y
PsbQ:96K
PsbQ:98K-PsbQ:133Y
PsbQ
PsbP:96K-PsbQ:1E
PsbP:115E-PsbP:173K
PsbP:93Y-PsbQ:1E
PsbP
PsbP:1A-PsbE:57E
PsbP:27K-PsbR:22D
PsbP:174K-CP26:96E
CP 26
PsbE
PsbR
B.
C.
20.4 Å
21.6 Å
11.4 Å
11.6 Å

Figure 10

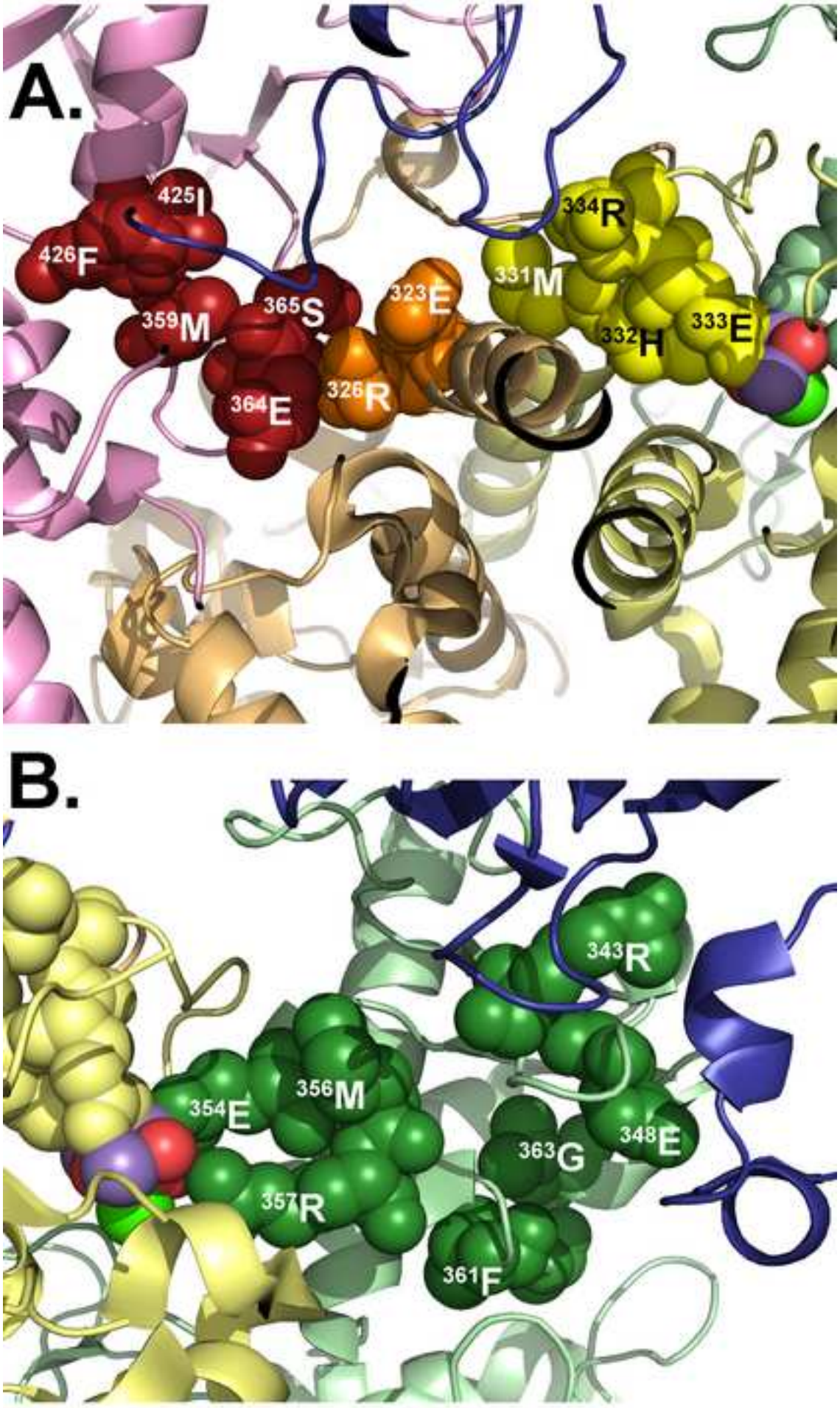
A.
425I
426F
359M
365S
364E
323E
326R
334R
331M
332H
333E
B.
343R
356M
354E
348E
363G
357R
361F

Figure 11

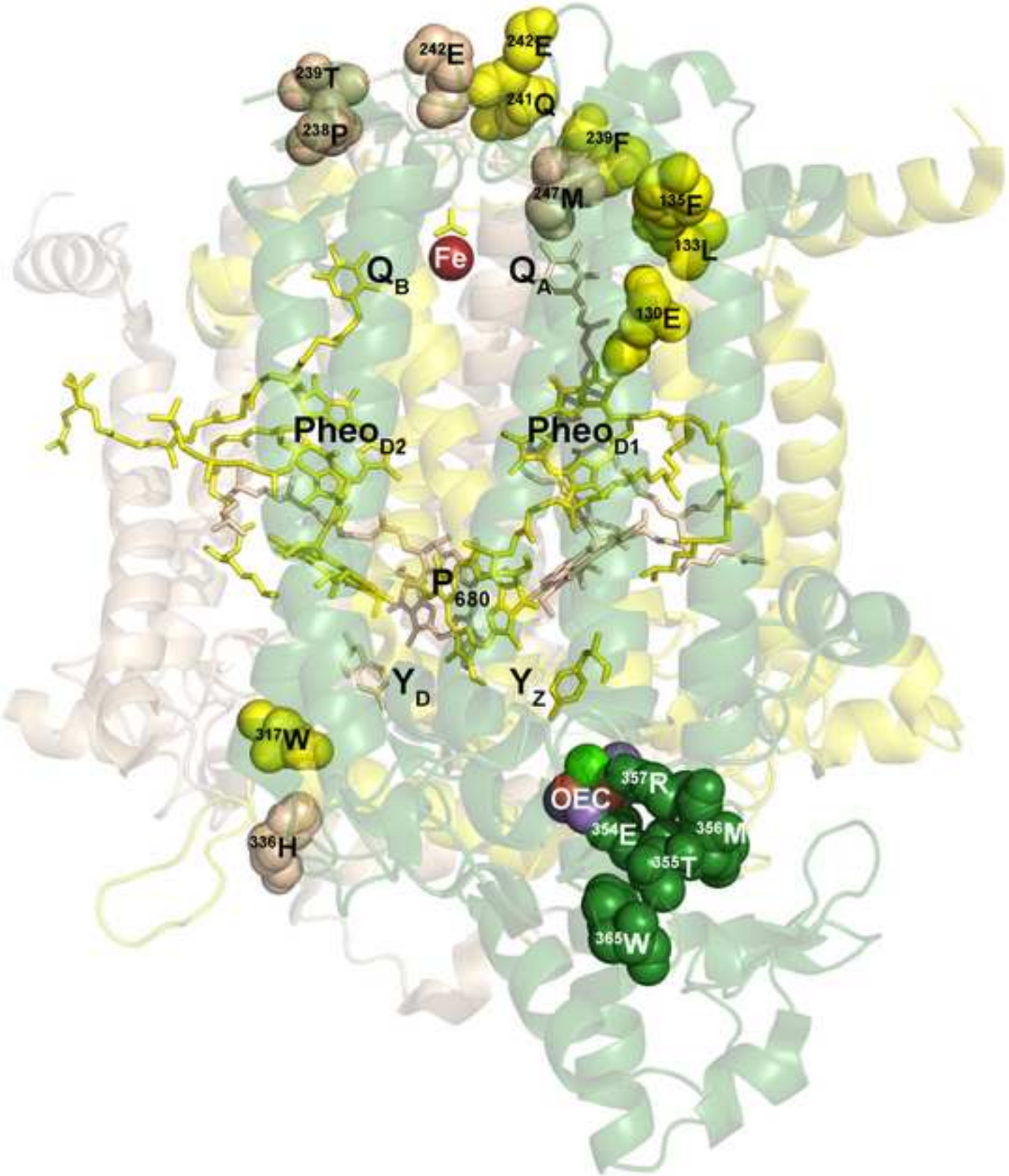
242E
242E
239T
241Q
238P
239F
247M
135F
133L
Fe
Q_B
Q_A
130E
$Pheo_{D2}$
$Pheo_{D1}$
P_{680}
Y_D
Y_Z
317W
OEC
357R
354E
356M
355T
336H
365W

Figure 12

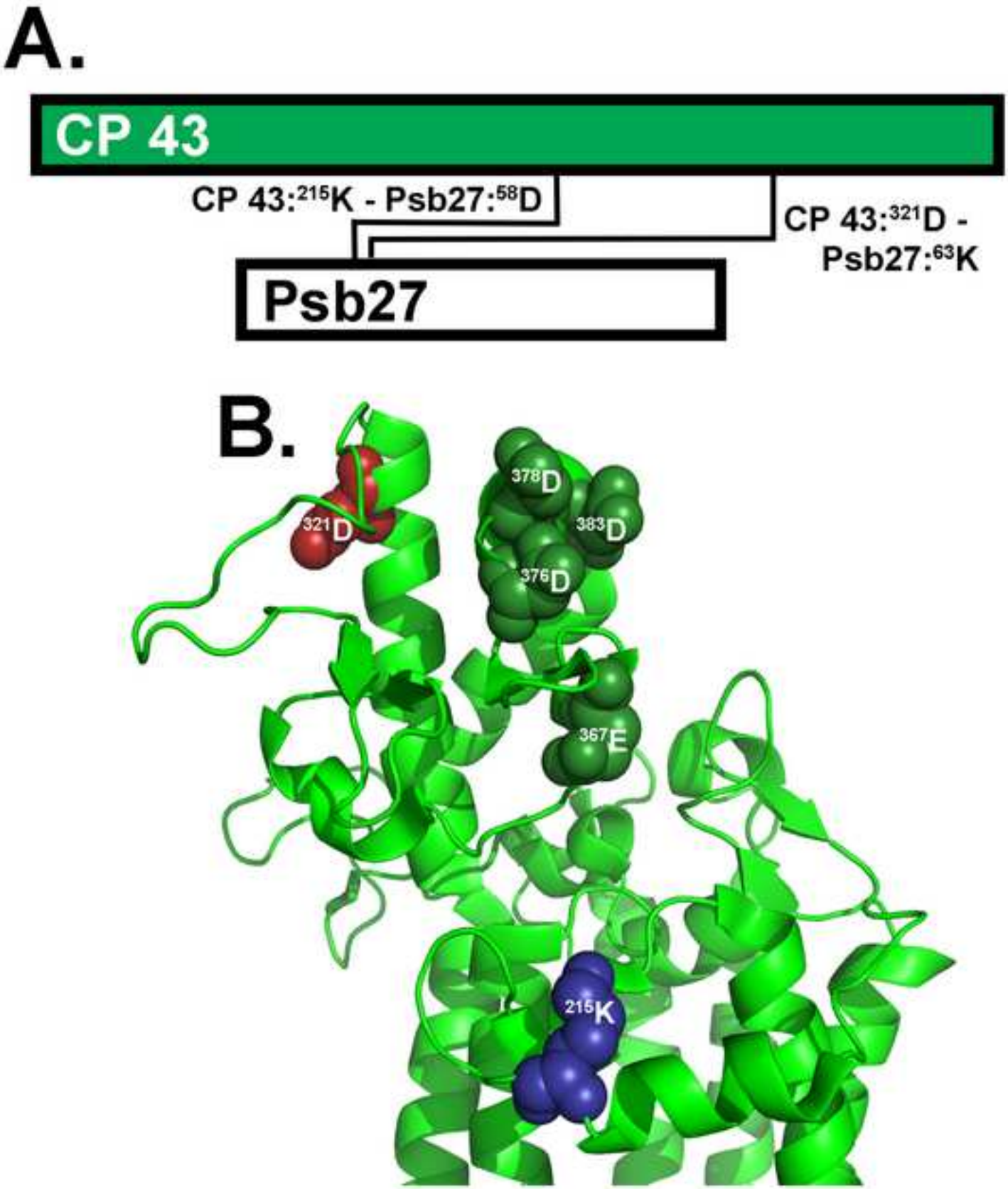
A.
CP 43
CP 43:215K - Psb27:58D
CP 43:321D - Psb27:63K
Psb27
B.
321D
378D
383D
376D
367E
215K

Table 1. [a]Mass Accuracies and Sensitivity of Modern Mass Spectrometers Used in Proteomics

Instrument Type	Mass Accuracy	Sensitivity
[b]FTICR	0.1 - 1 ppm	femtomole
Orbitrap	0.1 - 1 ppm	femtomole
TOF	1 - 5 ppm	femtomole
TQ	50-200 ppm	femtomole
LIT	50-200 ppm	femtomole

[a]These values are under optimal conditions. In practice, on real world peptides, observed mass accuracies are typically somewhat lower.

[b]FTICR, Fourier-transform ion cyclotron resonance, LTQ-Orbitrap; linear trap quadrapole; TOFMS, time-of-flight, time-of-flight; TQ, triple quadrapole; LIT, linear ion trap.